Amphibole: A major carrier of helium isotopes in crustal rocks

Journal Item

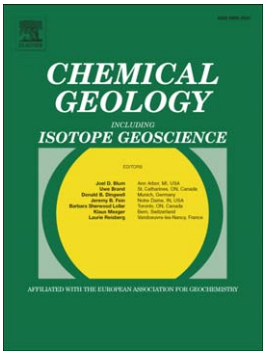

Amphibole: A major carrier of helium isotopes in crustal rocks

I.N. Tolstikhin, A.B. Verchovsky, I.L. Kamensky, V.I. Skiba, M.A. Gannibal, V.R. Vetrin, S.V. Tarakanov

PII: S0009-2541(16)30551-4
DOI: doi: 10.1016/j.chemgeo.2016.10.020
Reference: CHEMGE 18113

To appear in: *Chemical Geology*

Received date: 24 May 2016
Revised date: 6 October 2016
Accepted date: 9 October 2016

Please cite this article as: Tolstikhin, I.N., Verchovsky, A.B., Kamensky, I.L., Skiba, V.I., Gannibal, M.A., Vetrin, V.R., Tarakanov, S.V., Amphibole: A major carrier of helium isotopes in crustal rocks, *Chemical Geology* (2016), doi: 10.1016/j.chemgeo.2016.10.020

AMPHIBOLE: A MAJOR CARRIER OF HELIUM ISOTOPES IN CRUSTAL ROCKS

I.N. Tolstikhin[a,b,*], A.B. Verchovsky[c], I.L. Kamensky[a], V.I. Skiba[a], M.A. Gannibal[a], V.R. Vetrin[a], S.V. Tarakanov[d]

[a] Geological Institute, Kola Scientific Centre of Russian Academy of Sciences, Apatity, Russia;
[b] Space Research Institute, Russian Academy of Sciences, Moscow, Russia.
[c] The Open University, Milton Keynes, UK;
[d] The Laboratory of Glass Property, St. Petersburg, Russia

* Corresponding author at: Geological Institute, Kola Scientific Cantre RAS, Fersmana street 14, 184209, Apatity, Murmansk Region, Russia. Tel: 78155576769, FAX +7 81555 76481
E-mail address: <igor.tolstikhin@gmail.com>

Abstract

The first evidence for a specific role of amphiboles in He isotope balance of crustal rocks was presented in early contributions by Gerling et al. (1971, 1976). Since then it was shown that ^{4}He and ^{3}He concentrations in amphiboles generally exceed those in the host rock samples. Recently amphibole was considered as an important carrier of noble gases and other volatiles components in the course of their subduction into the mantle. This paper presents new data on the balance and mobility of noble gas isotopes and major gas constituents in amphibole separates in order to understand sources and evolution of volatile components of 2666 Ma old alkaline granites from Ponoy massif (Kola Peninsula), which underwent metamorphism 1802 Ma ago.

In the amphiboles ^{3}He, ^{4}He and ^{40}Ar* were dominantly produced *in situ* due to radioactive decay of the parent isotopes and associated nuclear reactions. A small fraction of He (≈ 3 % of the total) is liberated by crushing and shows ^{3}He /^{4}He ratio indistinguishable from that found by total extraction. The fraction of trapped ^{40}Ar* amounts to ≈ 40 %; both these fractions presumably occupy fluid inclusions and show rather low ^{4}He / ^{40}Ar* ≈ 0.1, a factor of ≈ 150 below the production ratio (calculated assuming no loss / gain of the species has happened since the time of metamorphism).

^{3}He has been better preserved in amphiboles compared with ^{4}He: the retention parameter (measured amount of He / totally produced amount) for ^{3}He (≈ 0.4) exceeds that for ^{4}He (≈ 0.15).

He extraction by fast and slow linear heating of amphiboles resulted in different release patterns. The fast heating (within 12 to 40 ^{O}C min^{-1}) revealed a superposition of two peaks. When heating with slower heating rate (below 8 ^{O}C min^{-1}) was applied, the high-temperature peak disappeared (the ”disappearing site”). Extractions of He atoms from grain and powder samples at different heating rates have shown: (1) the “disappearing site” is revealed by the fast heating analyses of different amphibole samples but not only those from the Ponoy massif; (2) amount of He liberated from the “disappearing site” is variable and generally much less than the total amount of He in the sample; (3) analysis of the powder produced in the crushing experiments never reveals the “disappearing site”; the temperature of He release from the powder is lower than that from the mm grain size sample by ≈50 ^{O}C. Possible explanations of the nature of the “disappearing site” are discussed. However, independently on nature of this effect, repeated gas extractions by heating at different rates would give additional information about structure and its transformation during heating of amphiboles.

The simplest explanation of the observed abundances of noble gas isotopes in the amphibole separates from Ponoy granites suggests local production, redistribution and partial loss of noble gases during evolution of the massif.

Keywords:
Isotope, Helium, Argon, Amphibole, Fluid inclusion, Granite

(1) Introduction

Noble gases are widely used as tracers of terrestrial fluids (Burnard, 2013). To understand sources and evolution of noble gas isotopes and thus shed light on the origin of other volatiles, a commonly used approach envisages comparison of measured abundances with those expected from production by radioactive decay and nuclear reactions. Thus, in case of He isotopes, measured concentrations of ^{4}He are compared with those that could have been accumulated by decay of U and Th (which concentrations are measured or estimated from *a-priory* data) within the time scale, known from, e.g., radiometric dating, stratigraphy, etc. The production ^{3}He / ^{4}He ratio is derived from modeling of nuclear reactions in the rocks (minerals) with known major and trace element composition, considering the ^{6}Li (n, α) ^{3}H → β- → ^{3}He nuclear reaction being the principal process for ^{3}He production (e.g., Morrison and Pine, 1955; Gorshkov et al., 1966).

Gerling et al. (1971) for the first time have demonstrated a very good agreement between measured and calculated production ratios of He isotopes (^{3}He/^{4}He = 1.45 × 10^{-8}) for a Rapakivi granite, Karelia,. This result was optimistically interpreted as evidence in favor of the approach, proposed by the above authors. However, later on Gerling et al. (1976) measured concentrations of parent elements, U, Th, Li, K, and daughter isotopes, ^{4}He, ^{3}He, ^{40}Ar* in minerals separated from the same Rapakivi sample (and several other rocks) and showed that the observed abundances of ^{3}He and ^{4}He in the mineral separates substantially deviate from the calculated production values because of highly variable retention of He isotopes by different minerals. In case of the Rapakivi granite, zircon (enriched in U and Th) and biotite (enriched in Li) appear to be the major producers of ^{4}He and ^{3}He, respectively. However, zircon and especially biotite readily loose the *in-situ* produced He, whereas amphibole, having relatively lower He isotopes production rate, contains much more ^{3}He and ^{4}He than zircon and biotite, since amphibole has the highest retention of these isotopes compared to other rock-forming minerals separated from the Rapakivi sample. Thus, the measured ratio of ^{3}He concentrations in amphibole (AM) to that in biotite (BT) and the corresponding production ratio (which is proportional to Li concentrations) in these minerals are: $^3He_{AM}$ / $^3He_{BT}$= 7.2 and Li_{AM} / Li_{BT}= 0.06, respectively, indicating a dramatically different ^{3}He retention (^{3}He /Li)$_{AM}$ / (^{3}He /Li)$_{BT}$= 120 in these minerals (see Section 4.3 for discussion). Later this has been confirmed by study of diffusivity of helium in amphiboles and micas (Lippolt and Weigel, 1988). It has also been shown that the different retention of He isotopes in minerals affects He isotope composition in related ground waters (e.g., Martel et al., 1990), emphasizing the importance of the noble gas production and retention study in the rock-forming minerals and in the rock-water systems (e.g., Tolstikhin et al., 2011).

Since the early papers by Gerling et al. (1971, 1976) a specific role of amphiboles in helium isotope balance of crustal rocks has been highlighted in several contributions (Table 1). The measured ^{4}He and ^{3}He concentrations in amphiboles always exceed those in the host rock samples and sometimes even those produced *in-situ* in amphibole via decay of U and Th and the related neutron-induced reactions. In some rocks (e.g., diorite gneiss, Table 1) balance of both He isotopes is mostly provided by the amphibole alone, in which case the direct comparison of the whole-rock measured and calculated ^{3}He /^{4}He ratios appears to be meaningless.

Table 1. Balance of He isotopes in whole rock samples and in amphiboles separated from these rocks

There are qualitative indications that sometimes He isotope abundances in amphiboles are associated with helium-rich pore waters. For instance, the high ^{4}He concentrations in amphibolites from the Kola Super-Deep borehole were observed within the interval, in which influx of ground waters into the drilling brine was detected (Kremenetsky et al., 1998). This interval was also marked by excess ^{4}He in quartz (Kremenetsky et al., 1998), similar to what was observed in the Molasses basin (Tolstikhin et al., 2011). Also, amphiboles often contain Ar trapped in fluid and melt inclusions (Kelley, 2002).

The excess (trapped) noble gases in minerals are used to study: (1) sources of the trapped noble gases and other volatiles (Graham, 2002; Burnard, edt, 2013); (2) the processes responsible for their trapping into minerals (Sherlock and Kelley, 2002; Baxter et al., 2002; Tolstikhin et al. 2011; Gannibal, 2012); (3) specific properties of minerals, such as permeability and solubility of noble gas atoms, activation energy of their release, volumes available for trapped fluids and others (Trull and Kurz, 1993; Baxter, 2003; Kamensky and Skiba, 2011; Tolstikhin et al., 2010, 2011).

Recently an important role of amphiboles and serpentinized rocks as carriers of halogens and noble gases in the process of noble gas subduction into the mantle was brought to attention (Kendrick et al., 2011; Jackson et al., 2013, 2015). With increasing pressure and temperature (PT), clay minerals of oceanic sediments could be re-crystallized into volatile rich amphiboles. Also amphiboles occur in rocks of sub-oceanic lithosphere.

The major objectives of this study are to identify sites of noble gas isotopes in a set of amphiboles, analyze abundances of noble gas isotopes and chemically active gases in each site, and outline evolution of the minerals as recorded by the abundances of the volatile species. The retention parameters of helium isotopes, ^{4}He and ^{3}He, are to be obtained and compared in order to understand the rate of their migration.

To do this we developed experimental procedures, allowing separate extraction and analysis of volatile components from different sites. A linear heating analysis is used for identification of the sites the volatile species are associated with. We applied step crushing in order to releases gases from fluid inclusions. The step heating technique was used to analyze the original (coarse grained) and powdered (by crushing) samples. The isotopic abundances of He, Ar and compositions of chemically active gases have been determined in the experiments.

Rocks and minerals of ancient (2666 Ma) Ponoy massif of alkaline granites (Kola Peninsula) were selected for this study with focus on amphiboles. The alkaline varieties of amphiboles, show enhanced Li content and thus high ^{3}He concentrations, suitable to study its origin and migration. Rocks of this massif underwent metamorphism 1802 Ma ago, so redistribution of noble gases among the co-existing minerals and their isotope abundances can be used to characterize this event.

(2) Archean alkaline granites, the Kola Peninsula (North East Baltic Shield)

The Ponoy massif of alkaline granites (land surface area ≈ 700 km^2) situated on the boundary between Keivy and Imandra-Varzuga structural zones, which position is controlled by a fault zone of North – West stretch (Fig. 1). The massif consists of aegirine - arfvedsonite granites and less abundant granosyenites, quartz syenites and lepidomelane granites. Major minerals of aegirine - arfvedsonite granites are plagioclase (31 %), quartz (31 %), K-Na feldspar (28 %), amphibole (5 %), aegirine (5 %).

Study of the amphiboles allowed conditions of melt crystallization, such as total pressure, composition of fluid phase and temperature, to be recovered. Amphibole is not stable in andesite magma at temperatures above 950 – 970 ^{O}C and pressures above 18 – 20 Kbar (Helz, 1982). In

the case of amphibole crystallization from water bearing (water above 5 %) acid magmas, the minimal pressure is approximately 1 Kbar. Post-magmatic or metamorphic amphiboles could be formed under lower pressures.

Amphiboles from the Ponoy massif are represented by their alkaline varieties, *i.e.*, arfvedsonite, ribekite, ferrowinchite, and show highly variable compositions even within the same rock sample. Table 2 presents chemical composition of two amphibole samples.

Table 2. Chemical composition of the amphiboles

The accessory minerals, titanite, allanite, brown zircon, monazite, apatite, fluorite, magnetite, ilmenite, britholite, astrophyllite are generally concentrated within domains enriched in mafic minerals, whereas transparent fine-grained zircon crystals are included in plagioclase grains. Optical microscopy studies of these zircons show that they consist of a core with zonal structure (about 80 to 90 % of the mineral grain) overlapped by a zircon shell (Fig. 1). The core / shell boundaries are sharp. The age of the zircon cores, 2666 ± 10 Ma, is considered as crystallization age of the granites (Vetrin and Rodionov, 2009).

Fig. 1. Zircons

Among dike bodies, related to the alkaline granites, there are inter-granite pegmatites, endo- and exso- contact silexites, and exso-contact pegmatites, formed (as generally considered, e.g., Belkov, 1958; Kalita, 1974) by crystallization of residual alkaline granitic melts, enriched in rare and volatile elements. The amphibole separates were collected for this study from a small (20 to 30 cm thick) quartz – fieldspar vein with ilmenite and amphibole inclusions.

The late Paleoproterozoic stage of Svekofennian tectono – magmatic activity caused metamorphism of the alkaline granites and related dike complexes. Temperature and pressure of this event approach 500 – 550 ^{O}C and 5-6 kbar respectively (Petrov, 1999). New mineral paragenesis was formed (zircon, titanite, monazite, etc.) and some isotopic chronometers (e.g., K-Ar, Rb-Sr) were re-set. U-Th-Pb dating of the zircon shells (Fig. 1) gives 1802 ± 22 Ma, accepted hereafter as the age of metamorphism (Vetrin and Rodionov, 2009).

(3) Experimental

Experimental studies of the samples were performed at the Open University, UK (hereafter OU) and at the Geological Institute, Kola Scientific Center, Russia (GI). Several extraction techniques were developed in both laboratories in order to identify different sites of trapped and *in situ* produced gases in minerals and to extract the gases from each site separately.

(3.1) Gas extraction by heating

Two different types of instruments were used to extract volatile species from the minerals (from unprocessed grains as well as from previously crushed samples) by heating. The first one is double–vacuum high-temperature (up to 1750^{O}C) furnace consisting of Mo crucible heated by Ta heating element (GI). Design of this furnace is very similar to that described by Staudacher et al. (1978) and Lippolt and Weigel (1988). The crucible is first heated to the highest temperature without sample and pumped out in order to obtain low background. Then a sample can be dropped from a special sample-holder (in which it can also be pre-heated) into the crucible. The results for He and Ar released from the original samples by total extraction are

presented in Table 3, except for the upper bolded line, which along with Table 4 and Fig. 3 show the results of step heating (sample 24/90).

The second type of the extraction equipment was designed for the linear heating experiments: a sample is first loaded into a sample holder line, evacuated for 1 to 2 hours, and then dropped trough a gate valve into the high-temperature double-wall (ceramic outside and quartz inside) furnace with SiC heating element, pre-heated to ≈ 200 ^{O}C under vacuum to remove absorbed species, and then heated up to 1400 ^{O}C. The heating rate can be pre-set and is regulated via computer controlled Eurotherm (OU). Similar design with stainless-steel crucible heated by a heating element made of a high-resistance wire (up to 1000 ^{O}C) and controlled by a thermo-regulator with Pt-PtRh thermocouple was used in GI. The results of gas extractions performed by the linear heating are presented in Fig. 4, 5 and 9. It has been assumed that each peak of the gas release corresponds to a separate site of volatile species in the minerals. However, our studies have shown that this assumption is not always valid (Sections 4.4, 4.6).

(3.2) Gas extraction by crushing

Crushing is another widely used method for gas extraction from minerals; it is considered that this approach allows gases occupying fluid inclusions and those in the lattice of minerals to be separated (Hilton et al., 1993; Matsumoto et al., 2002; Scarsi, 2000, and references therein). Two types of vacuum crushing equipment were used in this study.

(1) Crushing is performed by vibration of a (pumped out and sealed off) glassy ampoule with a sample (grain size ≈ 1 mm) and small (diameter 3 mm) iron balls inside (GI crusher). The mean grain size of the post-crushing powder is ≈ 50 μm. Then the ampoule is broken in vacuum and gases, liberated during crushing, are admitted into the inlet system of the mass spectrometers. ^{4}He and ^{40}Ar* amounts extracted by GI crushing from amphiboles are presented in columns 2 and 8 of the Table 3, respectively.

(2) A conventional whole stainless steel electro magnet vacuum crusher, similar to that presented by Scarsi (2000), was used for step-crushing with pre-set number of strokes (OU). A series of five computer-controlled solenoids around the crushing tube work in sequence to raise the magnetic crushing rod (with weight of about 80 g) inside the tube to about 20 cm height, before it is allowed to drop back down onto the sample. After few thousands of stokes the residual material has grain size of a few μm. The gases released during given number of strokes are held in the tube until they are transferred into the inlet system. The crusher is cleaned after every sample with fine sandpaper (to remove any ingrained material from the internal surfaces), and washed with acetone before being sonicated for 1 hour. After loading a sample the crusher is baking out under pumping for overnight at ~200 ^{O}C. The procedural blank of the crushing extraction is ~9×10^{-14} mol and ~1×10^{-13} mol for ^{4}He and ^{40}Ar respectively.
Results of OU crushing are presented in Figure 6 and discussed in Section 4.4.

(3.3) Mass spectrometry

Gases, extracted from minerals by methods described in Sections (3.1) and (3.2), were admitted into corresponding inlet systems and analyzed using different types of mass spectrometers. For chemical analyses all extracted gas was directly admitted to quadrupole mass spectrometers (CIS200 at GI and Hiden Analytical at OU). The mass spectrometers were not calibrated by the standard mixture of gases and the results can be used only for qualitative interpretation. For noble gas isotope analyses chemically active gases were removed in the inlet-purification lines, using cold traps and Ti-Zr or Ti-Al getters. Purified noble gases were separated into few fractions using cold traps filled with activated charcoal or molecular sieves, and then admitted into the mass spectrometers, operating either in static (for measurements of He and Ar isotope abundances in the course of step heating and crushing extractions) or in dynamic

(e.g., for measurements of He flow from minerals in the course of linear heating at GI) vacuum mode. At OU He flow during linear heating was determined along with other extracted gases without separation.

A magnetic sector mass spectrometer (MI 1201) was used for measurements of noble gas isotopic compositions and concentrations at GI. The mass resoluton of MI1201, ~ 1000, allows a complete separation of $^3He^+$ from hydrogen ions H_3^+ and HD^+. The sensitivity for He was 3 $\times 10^{-5}$ A torr^{-1}, high enough for measuring ^{3}He / ^{4}He ratios $\approx 10^{-8}$; the sensitivity for Ar was 2 $\times$ 10^{-4} A torr^{-1}. Before each run the mass spectrometer was calibrated with our laboratory standard that has ^{4}He/^{3}He and ^{4}He/^{20}Ne ratios 6.29 $\times$ 10^5 and 47, respectively, other isotopic and elemental ratios in this standard being the same as in the atmosphere. He and Ar concentrations were determined by the peak height method with an uncertainty of ±5% (1σ). Uncertainties in the ^{4}He/^{3}He and ^{40}Ar/^{36}Ar ratios for the standard measurements were within ±2 % and ±0.1 %, respectively. The analytical blanks were within 4.5 $\times$ 10^{-14} mol for both ^{4}He and ^{36}Ar.
At the Open University crushing and thermal (linear heating) analyses have been performed using Finesse complex. The 'Finesse' instrument is a custom-built mass spectrometer system, consisting of three static-mode mass spectrometers (one for carbon, one for nitrogen and argon, and a quadrupole for helium and neon), all linked *via* high vacuum lines to a common extraction device (furnace or crusher), sample inlet and gas clean-up sections (see Wright et al., 1988; Wright and Pillinger, 1989; Verchovsky et al., 1997.

(4) Results and discussion

(4.1) K-Ar systematics

To understand sources of ^{40}Ar* in the amphiboles, we compare its measured concentrations with those calculated assuming complete reset of the K-Ar system in the course of metamorphism, 1802 Ma ago (in accord with the Rb-Sr dating, Section 2). The comparison shows that all but one sample contain excess trapped ^{40}Ar*, which fraction, Δ^{40}Ar*= (^{40}Ar*$_{MEAS}$ – ^{40}Ar*$_{CALC}$) / ^{40}Ar*$_{CALC}$ approaches in average 0.39 (column 11, Table 3). Concentrations of ^{40}Ar*$_{CALC}$ were calculated by using K concentrations from Table 3, ^{40}K decay constants from Begemann et al. (2001) and 1802 Ma accumulation time. The measured ^{40}Ar /^{36}Ar ratios in the minerals are extremely high (Table 3). Because of that, it does not really matter what ^{40}Ar/^{36}Ar ratio to use for correction for trapped (atmospheric) Ar. The present day air ratio ^{40}Ar /^{36}Ar = 298.56 (Lee et al., 2006) was actually used. However, in the case of using the isotope composition of Ar in 1802 Ma old atmosphere (^{40}Ar /^{36}Ar ratios between 200 and 250, Tolstikhin and Marty, 1998; Pujol et al., 2013) the correction for the atmospheric Ar change the calculated amount of ^{40}Ar* by ≈ 2%, that is less than precision of measurements (Section 3) and thus does not affect significantly the Δ^{40}Ar*values (Table 3).

Neighbor minerals could be a source of the excess Ar. Thus, ^{40}Ar*, produced in K-Na-rich feldspars, which are abundant in the Ponoy alkaline granites (Section 2), had been released from this mineral during re-setting of K-Ar system and could be trapped by the low-K amphibole and especially into the co-existing ilmenite (the mineral with the lowest K concentration among those selected from the same dike), which K – Ar age approaches 6 Ga and from which about 85 % of the total ^{40}Ar* is liberated from this mineral by GI crushing (Tolstikhin et al., 2014).

Also, a fraction of argon, generated *in-situ* during pre-metamorphic history of the amphiboles, could partially survive metamorphism, e.g., migrate into fluid inclusions (which highly increase the total sink capacity, Baxter, 2003) of the same minerals. This source of ^{40}Ar* is in accord with the isotopic composition of He, liberated by crushing presumably from fluid inclusions in amphiboles (Section 4.4).

In both cases the trapped $^{40}Ar^*$ component is expected to be (at least partially) released along with the major fluid components (H_2O, CO_2, N_2) by crushing, in accord with Scarsi (2000), or by heating up to the decrepitation temperature. Indeed, ≈ 11 % of $^{40}Ar^*$, more than ^4He (see Footnotes to Table 3), was released by GI crushing of amphibole 24/90. Because the GI crushing generally destroys only a fraction of vesicles, a significant part of the excess $^{40}Ar^*$ could survive crushing. The OU crushing liberated from 20 to 40 % of $^{40}Ar^*$, which is in an agreement with $\Delta^{40}Ar^*$ shown in Table 3.

Table 3. He and Ar isotopes in amphiboles
Table 4. Results of step heating

The step heating extraction shows one major $^{40}Ar^*$ peak at ≈ 900 ^OC (Table 4). The low $^4He/^{40}Ar^* = 0.1$ in the gas, released at this temperature indicates that release temperature of ^4He is substantially lower than that for $^{40}Ar^*$ (in an agreement with different diffusivities of these species, e.g., Lippolt and Weigel, 1988; Baxter, 2010). According to Fig. 5 and 9, the chemically active volatile species are also released at 850 - 900 ^OC. The reasons for simultaneous release of trapped and *in situ* generated volatile species are discussed below in Section 4.7.

(4.2) U-Th-Li-^{4}He-^{3}He systematics: radiogenic in situ produced ^{3}He and ^{4}He

In contrast to the K-Ar systematics, the U-Th-^{4}He one does not show evidences for a substantial amount of trapped He in amphiboles. Assuming that the accumulation time corresponds to the age of Svekofenian metamorphism (1802 Ma), the average retention of ^4He in the two samples, for which U and Th concentrations were determined, is $m_4 \equiv {}^4He_{MEAS} / {}^4He_{CAL}$ ≈ 0.15 (see Footnotes to Table 3): almost all *in-situ* produced ^4He has been lost from these samples.

A small fraction (in average 3 ± 1 %) of the total measured ^4He amount is liberated by crushing and presumably occupies fluid micro-inclusions (five runs of He extraction by GI crushing from the amphibole samples were performed). The evidence favoring the *in situ* origin of He isotopes in amphiboles follows from the U-Th-Li-^{3}He systematics and comparison of ^4He and ^3He release patterns (see Fig. 2 and 3 below).

The measured $^3He/^4He$ ratios (Table 3) substantially, by a factor of ≈ 40, exceed the typical crustal value, ≈ 2×10^{-8}. Such observation is generally interpreted as a contribution of trapped mantle helium. However, amphiboles from the alkaline granites show quite high concentrations of Li (Table 3). Therefore before appealing to mantle helium, a contribution of in-situ produced $^3He_{CAL}$ must be estimated. Nucleogenic ^3He is mainly produced via ^6Li (n, α)$^3H \rightarrow$ β-(half life 12.2 a) $\rightarrow$ ^3He reaction and $^3He_{CAL} = \sigma_6 \times {}^6Li \times \Phi \times t$, where $\sigma_6 = 945 \times 10^{-24}$ cm^2 is the cross section of the above reaction (Gorshkov et al., 1966), $^6Li = 0.074 \times$ Li atoms cm^{-3} is the abundance of the light Li isotope, Φ is the thermal neutron flux, neutrons cm^{-2} day^{-1}, and t is the irradiation time, days (in our case t = 1802 Ma = 6.68×10^{11} days).

The neutron flux is calculated from the whole rock U, Th concentrations and the rock chemical composition (Morrison and Pine, 1955; Gorshkov et al., 1966; Mamyrin and Tolstikhin, 1984; Andrews, 1985). For the Ponoy alkaline granites the average (for the 1802 Ma age) neutron flux is Φ = 7.6 neutrons cm^{-2} day^{-1}. This value is typical for granitic rocks; for example it is close to the calculated (11 neutron cm^{-2} day^{-1}) and measured (13 neutron cm^{-2} day^{-1}) values for the Rapakivi granite (Gorshkov et al., 1966); the difference is due to a higher Th concentration in the Rapakivi granite (Table 1). The comparison of the measured and calculated neutron fluxes, performed by Gorshkov et al. (1966), indicates that the accuracy of these calculations is ≈ 30 %.

Assuming that (i) the time of the nucleogenic ^{3}He(Li) accumulation in amphiboles is equal to the age of metamorphism (as in the case of ^{4}He); (ii) the neutron flux, 7.6 n cm^{-2} day^{-1}, is constant within the alkaline rock domain, from which the amphibole-bearing rocks were collected, and applying Li concentrations from Table 3, we can calculate the total *in situ* produced ^{3}He concentrations, $^{3}He_{CAL}$, and the retention parameters for ^{3}He(Li), *i.e.*, $m_3 \equiv {}^{3}He_{MEAS} / {}^{3}He_{CAL}$, for each sample. The results (5th column, Table 3) show that all measured ^{3}He concentrations are below the calculated values, as in case of ^{4}He, indicating loss of nucleogenic ^{3}He from amphiboles during their post-metamorphism evolution.

A high (m_3 up to ≈ 0.5) and relatively constant retention of ^{3}He suggests a simple test for the origin of ^{3}He by comparing the measured ^{3}He concentrations with Li content in amphiboles (Table 3, Fig. 2). A reasonably good correlation between these two parameters, seen in Fig. 2, allows us to conclude that: (1) the above assumption regarding the constant neutron flux in the alkaline granites is valid; (2) a major fraction of ^{3}He in amphiboles has been produced *in situ*; the relatively high retention of helium-3 indicates a specific homogeneous distribution of Li in mineral grains (see discussion below). The *in situ* origin of the nucleogenic ^{3}He is also confirmed by GI crushing, during which only a small fraction of the total helium-3 (presumably occupying fluid inclusions) is liberated. Similar release patterns for ^{3}He and ^{4}He indicate mainly *in situ* origin of ^{4}He as well (Fig. 3).

Fig. 2. Correlation between Li and He-3
Fig. 3. Step heating extraction of He

It should be emphasized that the nucleogenic ^{3}He and radiogenic ^{4}He have partially been lost from the amphiboles in significantly different extent, the average m_3 exceeds m_4 by a factor between 2 and 3 (Table 3 and footnotes to this Table).

(4.3) Migration of He atoms, which have been lost from amphiboles: better retentions of ^{3}He than ^{4}He

He is commonly used as a tool to study structures, defects in different materials and specific features of the diffusion process (e.g., Shelby, 1971; Baxter, 2010). In general ^{4}He diffusion is expected to be slower than ^{3}He; therefore a better retention of ^{3}He than ^{4}He in the amphiboles is not a trivial result and an explanation is needed. In natural minerals radiogenic ^{3}H(^{3}He) and ^{4}He atoms are located within radiation tracks and the reverse mobility of the atoms means that either the track parameters are different or the tracks with ^{3}H(^{3}He) and ^{4}He are located in different structural positions within the amphibole grains, associated with multi-pass or multi-domain diffusivity (Baxter, 2010).

The energy liberated by α-decay of ^{238}U, ^{235}U and ^{232}Th series varies within 4 to 9 MeV that corresponds to α-particle stopping distances between 10 and 35 μm, depending on the recoil energy of the He nuclides and the material structure. The average energy is about 5.4 MeV and the corresponding average stopping distance is ≈ 20 μm (Farley et al., 1996). The exothermal ^{6}Li (n, α)^{3}H reaction yields the average energy of 4.8 MeV, similar to the above value for 4He; therefore, a similar average stopping distance is expected as well. Thus, the track parameters cannot affect He isotope retention significantly.

In contrast, specific features of the crystalline lattice and/or sites within it, where the parent isotopes are located, can result in a substantial difference in the retention of radiogenic He atoms. This was illustrated, for instance, by the extremely low retention of radiogenic He in micas (see Introduction). The α-particles stopping distances are comparable with thickness of one layer of Bt crystalline structure characterized by a perfect cleavage; therefore, most of α-tracks, produced in Bt, are "open" to the interlayer interstitial space and He atom can easily

migrate through this space out of the grain: the mean residence time of He atom in the open track at room temperature is rather short, ≈ 1 year (Tolstihin et al., 1999).

Such He behavior is not valid for amphiboles. Amphibole basic structure is a double chain of tetrahedra, and minerals with chain structures (e.g., berils, cordierites) are known (since early paper by Damon and Kulp, 1958) to preserve noble gases quite well. However, if the parent isotopes are located close to grain boundaries or fissures, the opened tracks can be produced stimulating fast loss of radiogenic He atoms.

Li atoms are supposed to be uniformly distributed within crystalline lattice of the amphiboles being included into it structure. Li^+ ion radius, 0.68 Å, is similar to those of Mg^+ (0.74 Å), Fe^{++} (0.8 Å) and Al^+ (0.57 Å), and Li isomorphism with these elements is often observed in Fe- Mg- rich minerals, including amphiboles. Therefore tracks, yielded by the $^6Li(n, \alpha)^3H$ reaction, have a high probability to remain within the amphibole grain. He atoms within these "closed" tracks are retained much better, than in the opened ones. Also the residence times of hydrogen and helium atoms in opened tracks are different: ≈ 600 years and ≈ 1 year, respectively (at room temperature, Tolstikhin et al., 1999). Correspondingly, ^3H atoms, precursors of ^3He, stay in the tracks, generated by the (Li,n) reaction, not less than ≈ 10 years (^3H half life), *i.e.*, 10 times longer than atoms of radiogenic ^4He. During this time the track could have been recovered and ^3He atom produced by ^3H decay is thus preserved better.

U and Th are the highly incompatible elements; they concentrated sometimes nearby mineral boundaries, along fissures, or as a thin film mineralization. Therefore, α-tracks, produced by U and Th decay, often cross the mineral surfaces or fissures. Inside mineral grains these elements often (but not always, e.g., Komarov et al., 1985) form micro-mineral inclusions and α-tracks form a star-like structure around these inclusions (Komarov, 1977). This stimulates loss of ^4He atoms: even if only one track in the structure is opened it also opens the others. ^4He atoms, occupying the opened tracks, are released independently on the thermal history of rocks within a year. Farley et al. (1996) modeled relationships between radiogenic ^4He loss and grain size and concluded that (U-Th)/He dating requires "either large crystals, or correction of measured ages for alpha particle ejection". However, according to early studies by Gerling and his colleagues (e.g., Gerling, 1961; Morozova and Ashkinadze, 1971; Ashkinadze, 1980), internal fissures within mineral grains (even if these grains are "large") is a common feature of rock forming minerals (e.g., see Fig. 8); therefore, α-particles could often reside in open tracks and readily escape from mineral grains. That is why the ^4He retention parameter is generally less than 0.2 in whole rock samples (Mamyrin and Tolstikhin, 1984).

(4.4) Unusual release patterns of He from amphibole: fast linear heating

At first glance the release pattern of ^4He and ^3He during step heating of the amphibole samples 24/90, shown in Fig. 3, indicates one major peak in the temperature range between 500 and 900 ^OC. However, taking into account a rather low resolution of such method, we applied the linear heating extraction (with heating rate 30 $^OC\ min^{-1}$) to this sample. In this case the ^4He release pattern displayed a superposition of two peaks: a smooth increase of ^4He release starting at 450 ^OC was followed by a sharp peak with maximum at ≈ 700 ^OC (Fig. 4). Hence, at least two sites of ^4He atoms can be identified from the experimental data.

To reveal relationships between the helium release patterns and heating rate, the linear heating with several different heating rates was applied (Fig. 4). At relatively high rates from 40 to 12 $^OC\ min^{-1}$ the superposition of the two peaks was reproduced. When the heating rate was decreased to 7.5 $^OC\ min^{-1}$, the sharp peak at ≈ 700 ^OC disappeared. These observations have been reproduced in both GI and OU laboratories. Fig. 5 presents the He release pattern for the heating rate of 6 $^OC\ min^{-1}$: almost all He is released as one smooth peak, but a small higher-

temperature (880 ^{O}C) one has also been observed. A small amount of He, released at ≈ 880 ^{O}C, is comparable with that released by GI crushing (footnotes to Table 3). It is important to note that chemically active gases (m/e = 44, 28, 16) are released at 880 ^{O}C during both slow and fast linear heating (Fig. 5, 9). The mechanism of gas release at this temperature is discussed in Section 4.7.

The "disappearing site" is not a unique feature of the investigated sample 24/90: similar He release patterns have been obtained for other amphibole samples, *e.g.*, from the Ponoy massif and from the Western Keivy structure (Kola Peninsula). ^{4}He fraction, released from the "disappearing site", appears to be variable (even for the same sample, Fig. 4). Many amphibole samples show release pattern with one peak independently on the heating rate, so the "disappearing sites" is not a general feature of amphiboles.

Fig. 4. Fast incremental heating of amphibole 24/90
Fig. 5. Slow incremental heating of amphibole 24/90: He and other gases

The linear heating of the powder, produced by GI crushing (Section 3), gives only one smooth He peak (independently of the heating rate) at a slightly lower (by ≈ 50 ^{O}C) temperature, compared to the uncrushed sample.

The GI crushing of the fast pre-heated (up to 600 ^{O}C) sample 24/90 (temperature was increased during 30 min from room temperature to 600oC, kept at 600 ^{O}C during 10 min, and then the sample was quickly cooled down) liberated approximately the same fraction of He, as during crushing of the original sample: ^{4}He = 7.6 × 10^{-10} mol g^{-1}, or 0.04 of the total amount (Section 4.2; footnotes to Table 3). The ^{3}He / ^{4}He ratio in helium released by crushing from the pre-heated sample, 127 (+/- 11) × 10^{-8}, was found to be similar to the bulk value, 118 × 10^{-8} (Table 3), and to that in helium liberated by crushing of the original sample, 104 (+/- 8) × 10^{-8}.

In the course of OU crushing of the sample 24/90 (Fig. 6), the ^{4}He/^{40}Ar* ratio is initially increasing (during, first few hundred strokes) due to mixing of gases with lower ^{4}He/^{40}Ar* (typical for fluid inclusions, see Footnotes to Table 3), and gases with ^{4}He/^{40}Ar* ≈ 2 (probably extracted from the lattice). The ^{4}He/^{40}Ar* is slightly decreasing as crushing proceeds, from 2 to 1.5. This decreasing trend is probably results from preferential release of movable ^{4}He relative to ^{40}Ar*from the lattice, so that the released gases are slightly depleted in helium in later crushing steps. According to Hilton at al. (1993), gases from crystalline lattice can be released during crushing if the total energy applied to the sample exceeds a certain threshold. This threshold depends on many parameters such as mineral structure, inclusion's size distribution, crusher construction.

During pre-heating up to 700 ^{O}C (at OU) a substantially larger fraction of ^{4}He was lost compared to that for ^{40}Ar*; therefore, the residual ^{4}He /^{40}Ar* ratio has been decreased (Fig. 6). However, the major result of the pre-heating is that during early stages of crushing of the preheated sample (first few hundred strokes) quite a large He fraction is liberated, ≈ 50 %, by ≈ 25 times larger than that released during crushing of the unheated sample. Also OU crushing of the pre-heated sample results in more significant decreasing of the ^{4}He / ^{40}Ar* ratio, by a factor of ≈ 3, than during crushing of the original sample (Fig. 6). This experiment shows that pre-heating generates specific sites, from which stimulates He is released faster.

Summarizing this section we can note that four sites of noble gas atoms are observed in the amphibole separates from the Ponoy massif: (i) fluid inclusions, containing a small fraction of He and a larger fraction of ^{40}Ar*; (ii) relatively large radiation defects, hosting radiogenic ^{4}He and ^{3}He atoms (α-tracks, which could be partially annealed, partially interconnected), (iii) point defects with in situ formed ^{40}Ar*); and (iv) "disappearing site", related to the heating rate of the samples.

Fig. 6. Extraction of ^{4}He and ^{40}Ar from unprocessed and pre-heated grains of amphibole by OU crushing.

(4.5) He migration in amphibole: a diffusion model

To understand the process of He migration in our samples and shed light on the "disappearing site" phenomenon we applied a diffusion model to the results (Fig. 5) obtained by linear heating .

The model considers He diffusion from a spherical grain (with radius *R*) under heating with known rate. Then the concentration of He atoms inside the grain is given by:

$$\partial_t C = \frac{D(T)}{r^2}\partial_r\left(r^2\partial_r C\right). \qquad (1)$$

In Eq. (1) the He concentration on the grain surface is considered to be equal to zero,

$$C\big|_{r=R} = 0, \qquad t > 0, \qquad (2)$$

and initial homogeneous concentration of He inside the grain is assumed:

$$C\big|_{t=0} = C_0, \qquad r < R. \qquad (3)$$

Parameters of Eq. (1) are: t is the running time; r is the radial coordinate, D is the diffusion coefficient, T is the temperature (a function of time) and C is the He concentration.

From Eq. (3) we derive the initial amount of He atoms in the grain, $M_0 = C_0\frac{4}{3}\pi R^3$,

and after diffusion has started, the amount of He in the grain is given by the integral:

$$M = 4\pi\int_0^R r^2 C\,dr.$$

The retention parameter, i.e., the fraction of gas remined in the grain, is expressed as

$$m(t) = \frac{M(t)}{M_0} = \frac{4\pi\int_0^R r^2 C\,dr}{\frac{4}{3}\pi R^3} = \frac{3}{R^3}\int_0^R r^2 C(r,t)dr, \qquad (4)$$

Correspondingly, the fraction of He released from the grain is:

$$g(t) = 1 - m(t), \qquad (5)$$

From Eq. (4) the fraction of He atoms, released from the grain, can be derived as:

$$d_t m = \frac{3}{R^3}\int_0^R r^2\partial_t C(r,t)dr = \frac{3D(T)}{R}\partial_r C\big|_{r=R}. \qquad (6)$$

The relation between the diffusion coefficient and the temperature is given by:

$$D = D_0 \exp\left(-\frac{E}{R_A T}\right), \quad (7)$$

where D_0 is the frequency factor, E is the activation energy; R_A is the universal gas constant.

Then we found the D_0 and E values, which give the best fit of the calculated and observed release patterns of ^{4}He (Fig. 7).

The diffusion parameters are compared (Table 5) with those obtained for another amphibole sample from a different locality (the Keivy massif), which is also characterized by the "disappearing site", as well as with published data (Lippolt and Weigel, 1988; Jackson et al., 2016). The amphiboles studied by Lippolt and Weigel (1988) were selected from eclogite (SAU B) and diorite (LK-5). Jackson at al. (2016) irradiated their gem quality samples by fast protons in order to generate ^{3}He and ^{21}Ne, which diffusion was investigated. The activation energies obtained for all the samples are similar, whereas the He release times vary within three orders of magnitude.

Jackson et al. (2016) considered relationships between occupancy of the ring site (or A site), a large-radius site in the crystalline structure of amphiboles (which can serve as a trap for migrating noble gas atoms), and the rate of He and Ne diffusion in the minerals. In case of an enhanced concentration of the large radius cations, potassium and sodium (in pargasite and richterite), this site is occupied thus stimulating fast release of He and Ne atoms from the samples. If concentrations of Na and K are low, the ring site is less occupied (actinolite and glaucophane) and open traps retard diffusion (Table 5). The amphiboles from the alkaline granites of the Ponoy massif show rather high concentrations of K and Na and fast release of He, in accord with results by Jackson et al. (2016). The compositions of other samples, presented in Table 5, are not known.

Fig. 7. Good fit between experimental release of He atoms and its approximation by calculations
Table 5. Diffusion parameters: a comparison

Taking into account (i) the good fit between calculated (using the diffusion model described above) and the observed release patterns (Fig. 7); (ii) the reasonable values obtained for the activation energy *E* and the He release time, comparable with other data, and (iii) the low-temperature He release: about ½ of the total He amount has been released before the dehydrogenation of amphiboles (see Fig. 9 and Section 4.7), we conclude that diffusion is the mechanism that provides He migration in amphiboles.

As will be discussed in Section (4.7), the decomposition of amphiboles occurs at ≈ 900 ^{O}C, whereas He release from the "disappearing sites" is observed at much lower temperature, ≤ 700 ^{O}C (Fig. 4, 9). So we assume that diffusion controls the release of He in both cases, during "slow" and "fast" heating (Section 4.4). It is also important that in the case of linear heating of the powdered samplers He is released at lower, (by ≈50 ^{O}C), temperature (Section 4.4), compared with temperature of He release from the uncrushed grains. Taking these issues into account, we suggest that the principal reason for the fast He release from the "disappearing sites" is decreasing of the diffusion radius during fast heating.

(4.6) The He "disappearing sites" in amphiboles

In principal, two parameters are responsible for the rate of He migration in minerals under given temperature: the structural and compositional properties of the mineral that collectively determine the activation energy and the rate of He release through the matrix, and

the He diffusion radius. Because the "disappearing site" phenomenon depends on the heating rate, these parameters should depend on the heating rate as well.

The reduction of diffusion radius could result from splitting up the grains due to the internal stress, caused by the large temperature gradients introduced by fast heating. However, preliminary estimates suggest that the temperature gradient arisen in a homogeneous grain (of 1 mm size or less) after it is gradually heated up (at rates ≈ 30 ^{O}C min^{-1}, see Fig. 4) is the highest at the beginning of heating and then continuously decreasing at higher temperatures. Therefore at the temperatures of He release from the "disappearing sites" (≈ 700 ^{O}C) the splitting due to thermal gradients appears to be unlikely. These estimates do not however take into account cleavage of the amphibole's crystalline lattice, which could stimulate splitting.

Amphibole heterogeneity, associated with the presence of mineral inclusions that already discussed in Sections 2 and 4.3, can also play a role: mineral micro inclusions such as quartz, microcline, apatite, ilmenite, magnetite and zircon are observed in alkaline amphiboles; size of these inclusions approaches tenths of microns (Fig. 8). Stresses within the amphibole grain could appear as a result of variable expansions of the crystalline lattices of amphibole and mineral inclusions and produce micro fissures providing path ways for fast escape of noble gas atoms.

Fig. 8. Inclusions in amphiboles

In the next section we consider chemical processes, which could modify properties of crystalline lattice of amphibole and thus stimulate fast He release.

(4.7) Amphibole behavior under vacuum heating and gas loss at ≈900 ^{O}C

Amphibole belongs to the mineral types which structure undergoes irreversible transformations at certain temperature in the course of heating under vacuum condition. First of all it is dehydrogenation: water reacts with iron to produce hydrogen, which is the main constituent of the gas release. Typical activation energies of amphibole dehydrogenation vary within 40 to 100 Kcal mol^{-1} range, and the temperatures are in the range from ≈ 600 to ≈ 1100 ^{O}C. Iron rich amphiboles show lower activation energies than magnesium rich ones (Gerling et al., 1966). The scale of dehydrogenation is recorded by weight loss of the mineral during vacuum heating, accompanied by the structural changes, which are manifested by decreasing unit cell dimensions with increasing temperature (Gaber et al., 1988). Fig. 9 illustrates dehydration of amphibole 24/90 during fast linear heating.

The "disappearing sites" could be related to processes of Fe^{2+} oxidation, which produces internal stresses in the crystalline structure of amphibole, especially within temperature interval around 600 to 800 ^{O}C (Lee, 1993); about ½ of the total amount of He in our samples was lost within this interval (Fig. 4, 5, 9). These stresses could generate a network of fast-diffusion pathways (micro cracks and fissures) and thus play an important role in the release of noble gases (Lee, 1993). The pathways are initial places of amphibole decomposition, also affecting noble gas loss (Lee et al., 1991). In the case of fast heating these stresses could be especially efficient and thus stimulate He loss from the "disappearing sites" at ≈ 700 – 800 ^{O}C (Fig. 4). The small spikes visible on the release patterns (curves m/e = 2, 18, 28, Fig. 9), appearing at ≈ 800 ^{O}C, could be related to the process responsible for He loss from the "disappearing sites".

A sharp decrease of hydrogen flux and loss of all volatile species takes place within a narrow temperature interval between 850 and 900 ^{O}C (Fig. 9). Chemically active gases, N_2, CO_2, presumably occupied fluid inclusions. However, *in situ* produced ^{40}Ar* is also partially released at these temperatures. The most adequate process, able to provide all these

observations, could be the amphibole decomposition. Lee et al. (1991) and Wartho et al. (1991) showed that bulk release of ^{40}Ar* from amphiboles occurs at temperatures correlated with the structural decomposition of the minerals. These temperatures depend on the amphibole compositions, first of all on the iron index Fe# = Fe_{TOTAL} / (Fe_{TOTAL} + Mg). Lee (1993) confirmed earlier studies by Gerling et al. (1966) and demonstrated a good correlation (for 27 samples) between Fe# and the temperature, at which a half of the total ^{40}Ar* has been lost. The correlation is regressed by $T_{1/2}$ = 1193 – 346 × (Fe#). The alkaline amphiboles from Ponoy massif are extremely Fe rich, with Fe# = 0.98 (Table 2), therefore the expected temperature of ½ × ^{40}Ar* loss is 850 ^{O}C. Taking into account some spread of the data points around the regression line (see Fig. 7 in Lee, 1993), the release of a half of ^{40}Ar* from the sample 24/90 at ≈ 900 ^{O}C fits the correlation quite well, and decomposition of our Fe-rich amphiboles at ≈ 900 ^{O}C or slightly above this temperature appears to be quite possible.

Fig. 9. Extraction of chemically active gases

More work is needed to understand the difference between He release from amphiboles under fast and slow heating. However, independently on the further studies, this result shows that the linear heating should be applied at several rates in order to identify noble gas sites in minerals and processes responsible for their migration.

(4.8) He, Ar isotopes and chemically active gases in the amphiboles from the Ponoy massif: sources and evolution

The abundances of helium and argon isotopes in the amphiboles along with the composition of chemically active gases (and geological data) recorded the sources and evolution of the volatile components in the Ponoy massif of alkaline granites.

The ^{3}He/ ^{4}He ratios, generally used to trace mantle fluids (e.g., Graham, 2002), can hardly identify a contribution of the mantle volatiles in the alkaline granites (and the amphibole separates) of the Ponoy massif. The high concentrations of Li in the amphiboles have resulted in enhanced ^{3}He/^{4}He (≈ 10^{-6} up to 2.05 × 10^{-6}) ratios in He of the samples. The measured concentrations of both He isotopes in amphiboles are well below those, produced *in situ* in these minerals during the post-metamorphism time interval (1802 Ma); hence, the major fraction of He isotopes has been lost. The amount of helium liberated by GI crushing and considered as released from fluid inclusions is rather small, ≈ 3 % of the total measured concentration (Table 3), and ^{3}He/^{4}He ratio in this "trapped" He is indistinguishable from that in the bulk sample, implying that "trapped" He has been produced in the amphibole.

In contrast to He, the average K-Ar age of the amphiboles exceeds the metamorphism age by ≈ 300 Ma (Table 3) and a substantial fraction of ^{40}Ar* is released by crushing. The amount of ^{40}Ar* in fluid inclusions exceeds the amount of He. This is indicated by the low ^{4}He/^{40}Ar* ratio in the gas liberated by crushing, ≈ 0.1 (sample 24/90, Table 3) which is by a factor of 30 below the bulk value and by 150 below the production ratio, 15. The amphiboles show rather high ^{40}Ar/^{36}Ar ratios, up to 56,000, indicating negligible contribution of the atmosphere-derived Ar_{AIR}.

The simplest explanation of all these observations suggests local production, redistribution and loss of noble gases in the course of evolution of the Ponoy alkaline granites (as has been proposed for several other localities by, e.g., Lee et al., 1990; Sherlock and Kelley, 2002; Baxter, 2003). The radiogenic ^{4}He, ^{3}He and ^{40}Ar* isotopes had been formed *in situ* in the amphiboles during the pre-metamorphic time interval (from 2666 to 1802 Ma ago). Before and during the metamorphic event He was released from these minerals preferentially to ^{40}Ar*; this

resulted in the low $^4He/^{40}Ar^*$ in the residual gases survived the metamorphic event and presently occupying fluid inclusions. As it follows from the observations (Mamyrin and Tolstikhin, 1984) and modeling (Tolstikhin et al., 2010) the fluid / mineral interface resistance to migration of noble gases from fluid inclusions is rather strong due to the low solubility of noble gases in matrix of silicate minerals. Therefore noble gases are generally quite well preserved in the inclusions and $^4He/^{40}Ar^*$ could be considered as "frozen" in there.

Even though hydrogen and water are the major component releasing from the amphiboles in the course of linear heating (Fig. 9), a contribution of air saturated ground water (carrier of noble gases with low ^{40}Ar / ^{36}Ar and high $^4He/^{40}Ar^*$ ratios) into the metamorphic fluid was rather limited. Large amounts of hydrogen (mass 2), which release pattern only partially correlates with those of the other gases, are released due to vacuum-heating-initiated dehydrogenation of the minerals (Gerling et al., 1966; Lee, 1993).

5. Conclusions

The investigation of U-Th-Li-^{4}He-^{3}He balance in minerals, which age is known, allows comparison of amounts of retained and released radiogenic species. The retention parameters of helium isotopes, which have been lost from amphiboles (separated from alkaline granites of the Ponoy massif, Kola Peninsula) are different: ^{3}He is preserved better than ^{4}He. This probably results from different location of the parent isotopes, U, Th and Li, in the mineral grains. Due to the high and relatively constant ^{3}He retention a reasonably good correlation between concentrations of ^{3}He and Li is observed, implying mainly radiogenic origin of ^{3}He. A similar release pattern of ^{4}He and ^{3}He indicates radiogenic origin of ^{4}He as well. Amount of He isotopes liberated by crushing is small, a few % of the total amount.

Our results highlighted the importance of applying of different extractions methods / conditions, if sites and mobility of noble gas isotopes in minerals are investigated. Under certain conditions experiment-induced sites can be formed. For example, fast and slow liner heating of the amphibole separates resulted in different helium release patterns. More work is required to understand what actually causes this phenomenon. It worth noting, that linear heating with different rates appears to be a useful method for study of He migration.

The combined study of sites and mobility of noble and chemically active gases appears to be useful for understanding the origin and evolution of the volatile species in the rocks. The active gases mainly reside in fluid inclusions, and if noble gases are liberated along with the active ones, they are also from the same inclusions. The isotope abundances of these noble gases shed light on the sources and evolution of chemically active ones. For instance, extremely high ^{40}Ar /^{36}Ar ratios along with low $^4He/^{40}Ar^*$, observed in fluid inclusions of the amphiboles, indicate "short-distance" redistribution of all volatile species among coexisting minerals in the course of metamorphism, without considerable contribution of ground-water-derived gases with high abundances of atmospheric species.

Simultaneous loss of all volatiles species from both gas-liquid inclusions (H_2O, CO_2, N_2) and matrix ($^{40}Ar^*$) along with a sharp drop of the hydrogen release within temperature interval from 850 to 900 ^{O}C are resulted from decomposition of the amphibole. This relatively the low decomposition temperature was provided by a high concentration of Fe in our samples, Fe# = 0.98, which accelerates destruction of the crystalline lattice in the course of vacuum heating.

Acknowledgements

This study was supported by grant 16-05-00756 of Russian Fond of Fundamental Research. The authors thank Ya. Pakhomovsky, L. Lialina, D. Lukanin and M. Vetrina for their help in preparing this contribution.
Careful, highly professional and constructive reviews by two anonymous Reviewers were extremely helpful and stimulated a substantial improvement of this paper.

References

Andrews, J. N., 1985. The isotopic composition of radiogenic helium and its use to study groundwater movement in confined aquifers. Chem. Geol. 49, 339-351.

Ashkinadze, G.Sh., 1980. Migration of radiogenic isotopes in minerals. Nauka, Leningrad, 144 pp..

Baxter, E.F., 2003. Quantification of the factors controlling the presence of excess ^{40}Ar or ^{4}He. Earth Planet. Sci. Lett. 216, 619-634.

Baxter, E. F., 2010. Diffusion of noble Gases in minerals. Rev. Miner. Geochem. 72, 509-557.

Baxter, D.J,. DePaolo, P.R., Renne, P.R., 2002. Spatially correlated anomalous 40Ar/39Ar 'Age' variations about a lithologic contact near Simplon Pass, Switzerland: A mechanistic explanation for excess Ar. Geochim. Cosmochim. Acta. 66, 1067-1083.

Begemann, F., Ludwig, K. R., Lugmair, G. W., Min, K., Nyquist, L. E., Patchett, P. J., Renne, P. R., Shih, C.-Y., Villa, I. M., Walker, R. J., 2001. Call for an improved set of decay constants for geochronological use. Geochim. Cosmochim. Acta 65, 111-121.

Belkov, I.V., 1958. Yttrium mineralization of amazonite pegmatites from alkaline granites of the Kola Peninsula. In: Problems of geology and mineralogy of the Kola Penunsula, 1, Nauka, Moscow 126-139 pp.

Burnard, P.E. (Ed.), 2013. The Noble Gases as Geochemical Tracers. Springer, Heidelberg, 391 pp.

Farley, K.A., Wolf, R.A., Silver, L.T., 1996. The effects of long alpha-stopping distances on (U-Th)/He ages. Geochim. Cosmochim. Acta. 60, 4223-4229.

Damon, P. E., Kulp, J. L., 1958. Excess helium and argon in beryl and other minerals. Amer. Mineral. 43, 433-459.

Gaber, L. J., Foland, K. A., Corbato, C. E., 1988. On the significance of argon release from biotite and amphibole during vacuum heating. Geochim. Cosmochim. Acta 52, 2457-2465.

Gannibal, M.A., 2012. Equilibrium partitioning of helium between rock and pore water: new approach for dating of old ground waters. Geokhimiya, 1, 1-12.

Gerling, E.K., 1961. Present-day status of argon method of age determination and its application in geology. SSSR Academy of Sciences, Moscow, 75 pp.

Gerling, E.K., Petrov, B.V., Koltsova, T.V., 1966. **A** comparative study of the activation energy of argon liberation and dehydration energy in amphiboles and biotites. Geochimica Intl. 3,295-305.

Gerling, E.K., Mamyrin, B.A., Tolstikhin, I.N., Yakovleva, S.S., 1971. Helium isotopic composition in some rocks. Geochimiya 10, 1209-1217.

Gerling, E.K., Tolstikhin, I.N., Drubetskoy, E.R., Levkovsky, R.Z., Sharkov, E.V., Kozakov, I.K., 1976. Helium and argon isotopes in rock-forming minerals. Geochimiya 11, 1603-1611.

Gorshkov, G.V., Zjabkin, V.A., Ljatkovskaya, N.M., Tsvetkov, O.S., 1966. Natural neutron background of atmosphere and Earth's crust. Atomizdat, Moscow, 410 pp.

Graham, D.W., 2002. Noble gas isotope geochemistry of mid-ocean ridges and ocean island basalts: characterization of mantle source reservoirs. In: Noble gases in geochemistry and

cosmochemistry. D. Porcelli, Ballentine, C.J., Wieler, R. (ed.), Mineral. Soc. Amer. 47, 247-318.

Helz, R.T., 1982. Phase relations and composition of amphiboles produced in studies of the melting behavior of rocks. Reviews in Mineralogy 9B, 279-347.

Hilton, D. R., Hammerschmidt, K., Teufel, S., Friedrichsen, H., 1993. Helium Isotope Characteristics of Andean Geothermal Fluids and Lavas. Earth Planet. Sci. Lett. 120, 265-282.

Jackson, C.R.M., Parman, S.W., Kelley, S.P., Cooper, R.F., 2013. Noble gas transport into the mantle facilitated by high solubility in amphibole. Nat. Geosci. 6, 562-565.

Jackson, C. R. M., Parman, S. W., Kelley, S. P., Cooper, R. F., 2015. Light noble gas dissolution into ring structure-bearing materials and lattice influences on noble gas recycling. Geochim. Cosmochim. Acta 159, 1–15.

Jackson, C. R. M., Shuster, D. L., S.W., P., and Smye, A. J., 2016. Noble gas diffusivity hindered by low energy sites in amphibole. Geochim. Cosmochim. Acta 172, 65-75.

Kalita, A.P., 1974. Pegmatites and hydrothermalites of the alkaline granites, Kola Peninsula. Nauka, Moscow 140 pp.

Kamensky, I.L., Skiba, V.I., 2011. Determination of genesis of fluid inclusions in minerals by using helium and argon isotopes. Geokhimiya 1, 50-58.

Kamensky, I. L., Tolstikhin, I.N., Vetrin, V. R., 1990. Juvenile helium in ancient rocks: I. ^{3}He excess in amphiboles from 2.8 Ga charnokite series - Crust-mantle fluid in intracrustal magmatic processes. Geochim. Cosmochim. Acta 54, 3115-3122.

Kelley, S., 2002. Excess argon in K–Ar and Ar–Ar geochronology. Chem. Geol. 188, 1 – 22.

Kendrick, M.A., Scambelluri, M., Honda, M., Phillips, D., 2011. High abundances of noble gas and chlorine delivered to the mantle by serpentinite subduction. Nature Geosci. 4, 807-812.

Komarov, A.N., 1977. Sites of U atoms in some minerals used for U-Pb dating, in: Shukolyukov, Yu.A. (Ed.), Problems of dating of Precambrian formations. Nauka, Leningrad, 225-235 pp.

Komarov, A.N., Berman, I.B., Koltsova, T.V., 1985. Radiographic study of distibution of uranium and thorium in granulites. Geokhimiya 7, 979-987.

Kremenetsky, A.A., Ikorsky, S.V., Kamensky, I.L., Sazonov, A.M., 1998. Geochemistry of deep crustal strata. In: Orlov V.P., Laverov H.P.(Eds), Kola super-deep borehole (scientific results and study experience) Nauka, Moscow, 71-98 pp.

Lee, J.K.W., 1993. The argon release mechanisms of hornblende in vacuo. Chem. Geol. 106, 133-170.

Lee, J.K.W., Onstott, T. C., Hanes, J. A., 1990. An 40Ar/39Ar investigation of the contact effects of a dyke intrusion, Kapuskasing structural zone, Ontario: A comparison of laser microprobe and furnace extraction techniques. Contrib. Mineral. Petrol. 105, 87-105.

Lee, J. K. W., Onstott, T. C., Cashman, K. V., Cumbest, R. J., Johnson, D. J., 1991. Incremental heating of hornblende in vacuo: Implications for 40Ar/39Ar geochronology and the interpretation of thermal histories. Geology 19, 872-876.

Lee, J.-Y., Marti, K., Severinghaus, J. P., Kawamura, K., Yoo, H.-S., Lee, J. B., Kim, J. S., 2006. A redetermination of the isotopic abundances of atmospheric Ar. Geochim. Cosmochim. Acta 70, 4507–4512.

Lippolt, H. J., Weigel, E., 1988. ^{4}He diffusion in ^{40}Ar-retentive minerals. Geochim. Cosmochim. Acta 52, 1449-1458.

Mamyrin, B.A., Tolstikhin, I.N., 1984. Helium isotopes in nature. Elsevier Sci. Pub., Amsterdam 273 pp.

Martel, D.J., O'Nions, R.K., Hilton, D.R., Oxburgh, E.R., 1990. The role of element distribution in producttion and release of radiogenic helium: the Carnmenellis Granite, southwest England. Chem. Geol. 88, 207-221.

Matsumoto, T., Seta, A., Matsuda, J., Takebe, M., Chen, Y., and Arai, S., 2002. Helium in the Archean komatiites revisited: significantly high 3He/4He ratios revealed by fractional crushing gas extraction. *Earth Planet. Sci. Lett.* **196**, 213-225.

Morozova, I.M., Ashkinadze, G.S., 1971. Migration of rare gas atoms in minerals. Nauka, Leningrad, 120 pp.

Morrison, P., Pine, J., 1955. Radoigenic origin of the helium isotopes in rock. Annals New York Acad. Sci. 62, 69-92.

Petrov, V.P. 1999. Early Proterozoic metamorphism of the Baltic Shield. Kola Scientific Centre RAS, Apatity, 325 pp.

Pujol, M., Marty, B., Burgess, R., Turner, G., Philippot, P., 2013. Argon isotopic composition of Archaean atmosphere probes early Earth geodynamics. Nature 498, 87-92.

Scarsi, P., 2000. Fractional extraction of helium by crushing of olivine and clinopyroxene phenocrysts: Effects on the $^{3}He/^{4}He$ measure ratio. Geochim. Cosmochim. Acta 64, 3751-3762.

Shelby, J. E., 1971. Diffusion of helium isotopes in vitreous silica. Phys. Rev. B4, 2681-2686.

Sherlock, S., Kelley, S.P., 2002. Excess argon evolution in HP-LT rocks: a UVLAMP study of phengite and K-free minerals, NW Turkey. Chem. Geol. 182, 619 - 636.

Staudacher, T., Jessberger, E. K., Dorflinger, D., Kiko, J., 1978. A refined ultrahigh-vacuum furnace for rare gas extraction. J. Phys. E: Sci. Instrum. 11, 781-784.

Tolstikhin, I. N., 1978. A review: Some recent advances in isotope geochemistry of light rare gases. In: Terrestrial Rare Gases. Alexander, E. C., Jr., M. Ozima (Ed.), Center for Academ. Publ, Japan, Tokyo, 33-62 pp.

Tolstikhin, I. N., Marty, B., 1998. The evolution of terrestrial volatiles: A view from helium, neon, argon and nitrogen isotope modelling. Chem. Geol. 147, 27-52.

Tolstikhin, I.N., Lehmann, B.E., Loosli, H.H., Kamensky, I.L., Nivin, V.A., Orlov, S.P., Ploschansky, L.M., Tokarev, I.V., Gannibal, M.A., 1999. Radiogenic helium isotope fractionation: The role of tritium as 3He precursor: geochemical applications. Geochim. Cosmochim. Acta. 63, 1605-1611.

Tolstikhin, I., Kamensky I.L., Tarakanov, S., Kramers, J., Pekala, M., Skiba, V., Gannibal, M., Novikov, D., 2010. Noble gas isotope sites and mobility in mafic rocks and olivine. Geochim. Cosmochim. Acta. 74, 1436–1447.

Tolstikhin, I., Waber, H. N., Kamensky, I.L., Loosli, H.H., Skiba, V., Gannibal, M., 2011. Production, redistribution and loss of helium and argon isotopes in a thick sedimentary aquitard-aquifer system (Molasse Basin, Switzerland). Chemical Geology 286, 48–58.

Tolstikhin, I.N., Skiba, V.I., Sevost'yanov, A.Yu., Kamensky, L.L., Vetrin, V.R., 2014. Sites and origin of noble gases in minerals (using ilmenite from alkalint granites, Kola Peninsula, as example). Geokhimiya 12, 1099- 1107.

Trull, T.W., Kurz, M.D., 1993. Experimental measurements of He-3 and He-4 mobility in olivine and clinopyroxene at magmatic temperatures. Geochim. Cosmochim. Acta 57, 1313-1324.

Verchovsky, A.B., Fisenko, A.V., Semjonova, L.F., Pillinger, C.T., 1997. Heterogeneous distribution of xenon-HL within presolar diamonds. Meteoritics Planet. Sci. 32, A131–A132.

Vetrin, V.R., Kamensky, I.L., Bayanova, T.B., Timmerman, M., Belyatsky, B.V., Levsky, L.K., Balashov, Y.A., 1999. Melanocratic enclaves and petrogenesis of alkaline granites of the Ponoy Massif (Kola Peninsula). Geochimiya 11, 1178-1190.

Vetrin, V.R., Rodionov, N.V., 2009. Geology and geochronologyof neoArchaean anorogenic magmatism of Keivy structure, Kola Peninsula. Petrology 17, 578-600.

Wartho, J., Dodson, M. H., Rex, D. C., Guise, P. G., Knipe, R. J., 1991. Mechanisms of Ar release from Himalayan metamorphic hornblende. Am. Mineral. 76, 1446-1448.

Wright, I.P., Pillinger, C.T., 1989. C isotopic analysis of small samples by use of stepped-heating extraction and static mass spectrometry. In: New frontiers in stable isotopic research: laser probes, ion probes and small sample analysis, Shanks, W.C., Criss, R.E. (Eds.), U.S. Geol. Surv. Bull. 1890, 9–34.

Wright, I.P., Boyd, S.R., Franchi, I.A., Pillinger, C.T., 1988. Determination of high precision N stable isotope ratios at the sub-nanomole level. J. Phys. E: Sci. Instrum. 21, 865–875.

Figure Captions

Fig. 1. Zircon crystals from alkaline granites, Ponoy massif, Kola Peninsula.
Cores of the zircons (zoning of gray colors) are covered by shells (black). U-Th-Pb isochrone dating of the cores and shells was performed by using SHRIMP (Karpinsky Geological Institute, St. Petersburg). The core age, 2666 ± 10 Ma, is considered as the age of crystallization of the alkaline granites; the shell age, 1802 ± 22 Ma, is considered as the age of metamorphism (Vetrin and Rodionov, 2009).
The inset shows position of the Ponoy massif (dark gray oval) within the main tectonic structures (megablocks) of the Kola Peninsula: (I) Murmansk, (II) Kola–Norwegian, (III) Keivy, and (IV) Imandra–Varzuga paleorift.

Fig. 2. Relationships between Li concentration, measured and calculated ^{3}He concentrations in amphiboles.
Except for one data point, a good linear regression is observed between the two parameters for the measured ^{3}He concentration; the regression equation and the coefficient of determination are shown in the plot. Correlation between Li and calculated ^{3}He concentration, corresponding to complete retention of ^{3}He, is shown on the top for comparison (circles).

Fig. 3. Step heating extraction of ^{4}He and ^{3}He from amphibole 24/90
The total amounts released are shown for each curve (mol).
Notice similar release patterns for ^{4}He and ^{3}He atoms.

Fig. 4. Extraction of ^{4}He from grains of amphibole 24/90 by linear heating.
The numbers next to the curves show the heating rates [^{O}C min^{-1}]. The sample-weights and the total amounts of He released were different in each run. Under fast heating (from 40 to 12 ^{O}C min^{-1}) He release pattern includes a smooth lower-temperature peak following by sharp higher-temperature one (hereafter termed as He release from the "disappearing site"). Under slow heating (e.g., 7.5 ^{O}C min^{-1} and below) almost all He is released as one peak: the sharp high-temperature peak disappears.
The inset shows two "end-member" interpretations of the two-peak release pattern, with high (dotted curves) and low (gray curves) fractions of He released from the "disappearing site". Note that these fractions are different in different runs.

Fig. 5. Extraction of ^{4}He (curve with m/e = 4) and chemically active gases, CO_2 (44), CO-N_2 (28), CH_4 (16) and C (12) from the amphibole 24/90 by slow linear heating.
The release amounts are measured in counts per second (CPS). Notice two residence sites of ^{4}He atoms. (1) The major fraction of He is released as a smooth peak under 650 ^{O}C; (2) a small peak of ^{4}He releasing at 880 ^{O} (hereafter high-temperature peak) corresponds to the ^{4}He amount, which is comparable with that liberated by GI crushing (≈ 0.03 × total observed amount). The peaks of chemically active gases were released in both cases, fast and slow heating, at the same (≈ 880 ^{O}C) temperature.

Fig. 6. Variations of the ^{4}He / ^{40}Ar* ratio in the course of OU crushing versus the cumulative yield of ^{4}He.
The solid and dashed curves correspond to the unprocessed and pre-heated to 700 ^{O}C samples of the amphibole 24/90, respectively. The numbers next to the data-points show the cumulative

fraction of ^{4}He extracted (%); the total concentration, 2.27×10^{-8} mol g^{-1}, is the average value from Table 3.

(1) While amount of He, extracted from the unprocessed sample, is below ≈ 3 % of the total, *i.e.*, very similar to that extracted by GI crushing, mixing of noble gases from different sources is observed: the first one shows a low ^{4}He/^{40}Ar* = 0.5, which is similar to that in gases liberated by GI crushing (Footnote to Table 3); the second one is represented by gases with ^{4}He/^{40}Ar* = 2; this ratio is slightly below the bulk value (3) in this sample (Table 3); the difference could be due to heterogeneity of the sample, as only 27 mg of amphibole separate was used for crushing. In the course of crushing the ratio is slightly decreasing, from 2 to 1.5, probably due to preferential loss of He in the previous crushing steps.

(2) During pre-heating the sample has lost He preferentially to Ar as reflected by the lower (by a factor of 2) ratio of ^{4}He/^{40}Ar*. However, the major result of pre-heating is a redistribution of both He and Ar into the sites that easily liberate gases under crushing: the first 1000 strokes liberated a large fraction of He, ≈ 50 %, much larger than that released from the un-processed sample (≈ 2.5 %). Also notice a large decrease of ^{4}He/^{40}Ar* ratio (with one exception) in the course of crushing, by a factor of 3.

Fig. 7. The diffusion parameters (shown in the plot for the grain size 1 mm) are those giving the best fit between the calculated (curve) and observed (circles, derived from Fig. 5) cumulative release of ^{4}He in the course of linear heating.

Fig. 8. Electron microscope image of amphibole 30/90.
Note a large (≈ 60 μm) quartz inclusion is in the right-bottom corner (dark oval). Other minerals, seen in this image, are microcline, ilmenite, rutile. Numerical fissures crossing the grain can also be seen.

Fig. 9. Extraction of chemically active gases by linear heating of the amphibole sample 24/90. The numbers next to the curves show m/e ratio, corresponding to H_2 (m/e = 2), H_2O (18), N_2 (28), CO_2 (44). The ^{4}He and ^{40}Ar* release pattern are added for comparison from Fig. 5 and Table 4, respectively.
Note an intense hydrogen release, related to dehydrogenation of amphibole, and simultaneous loss of all chemically active species and ^{40}Ar* at ≈ 900 ^{O}C, associated with decomposition of the mineral.

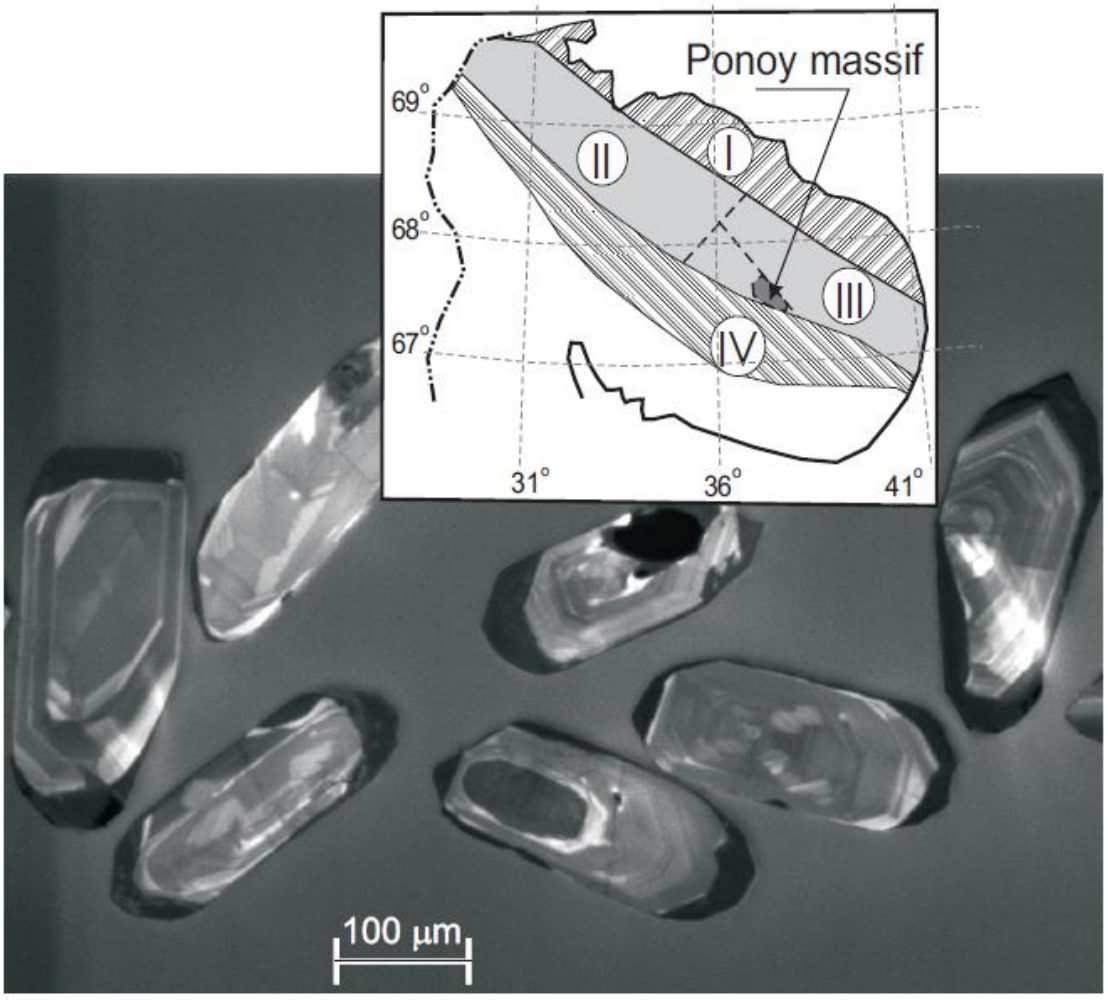

Figure 1

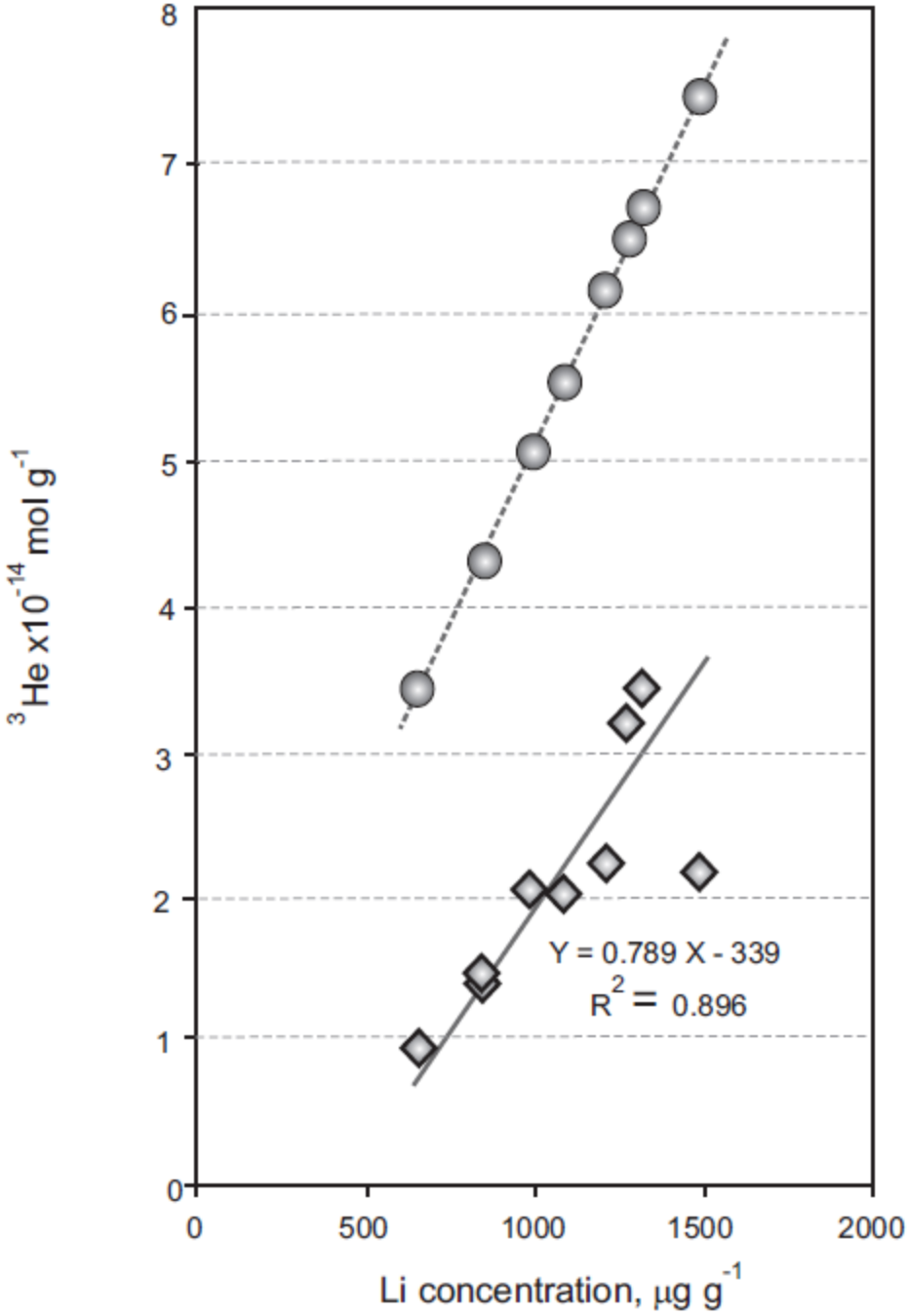

Figure 2

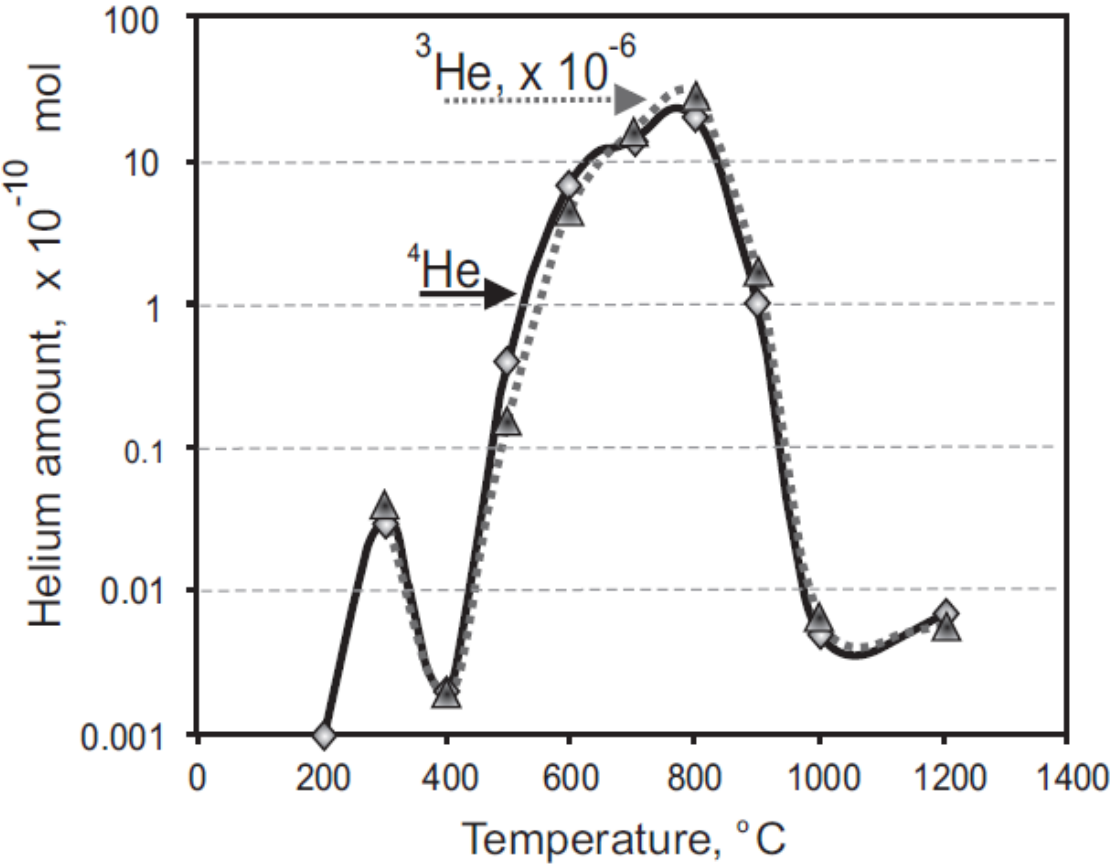

Figure 3

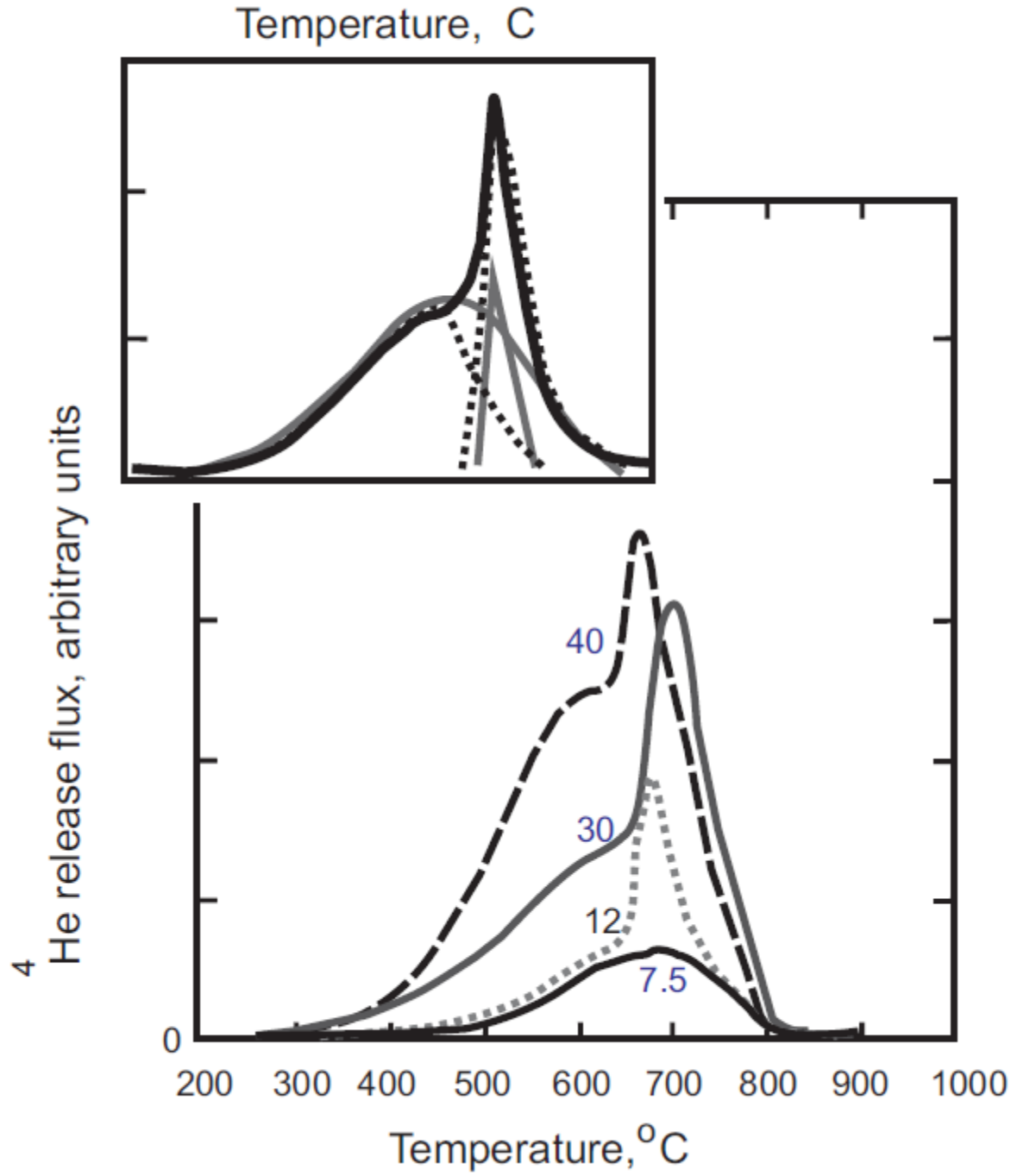

Figure 4

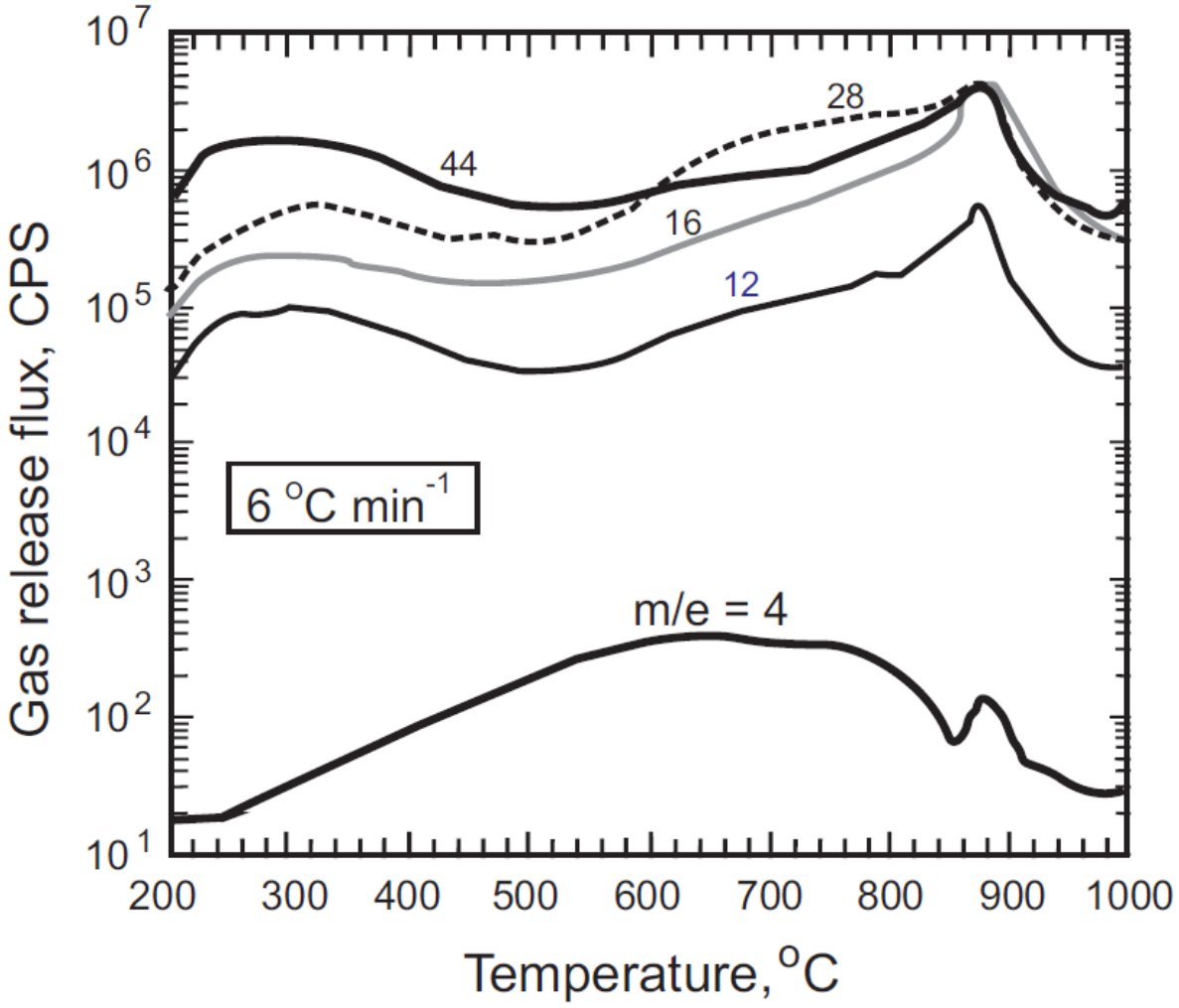

Figure 5

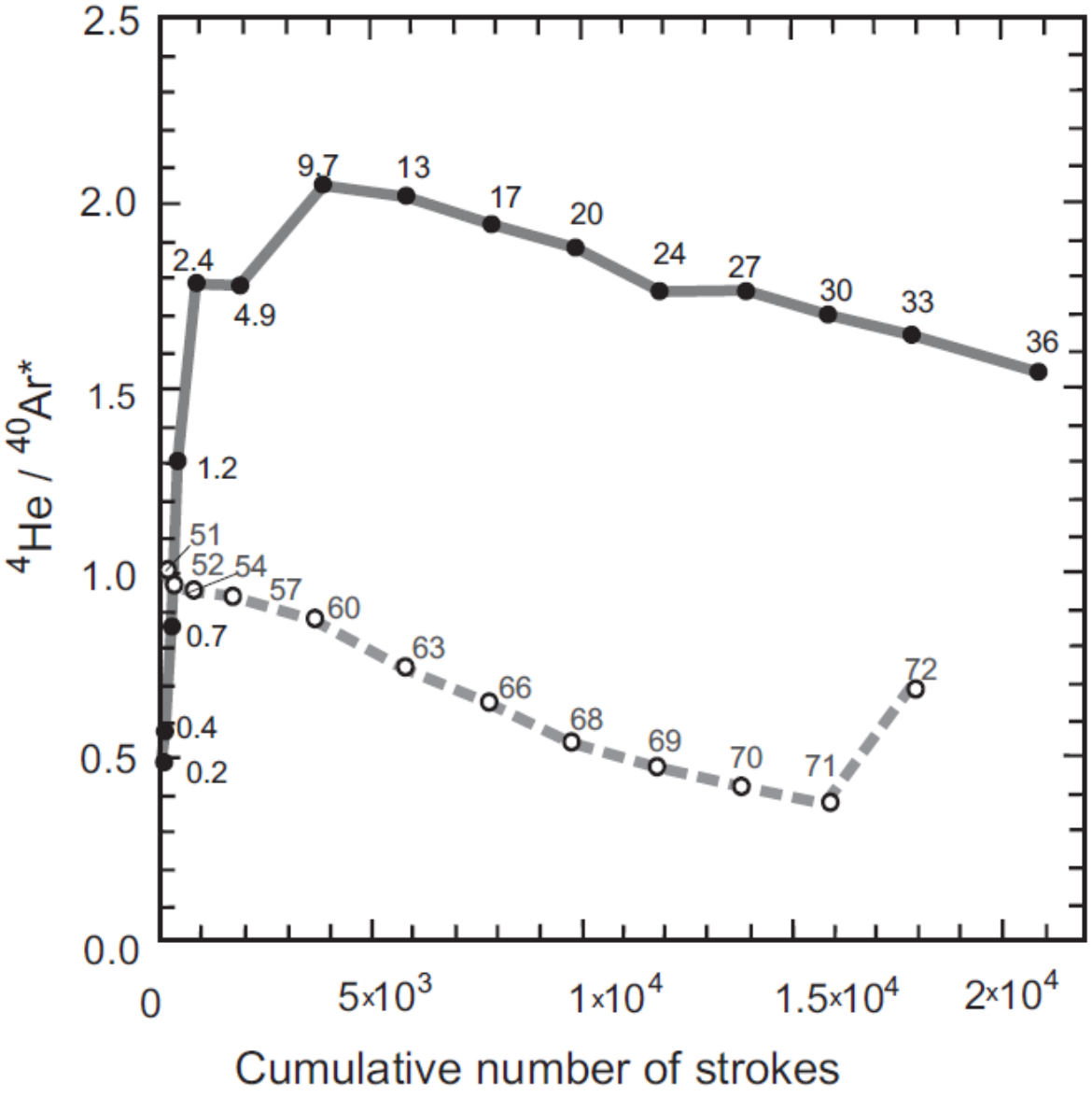

Figure 6

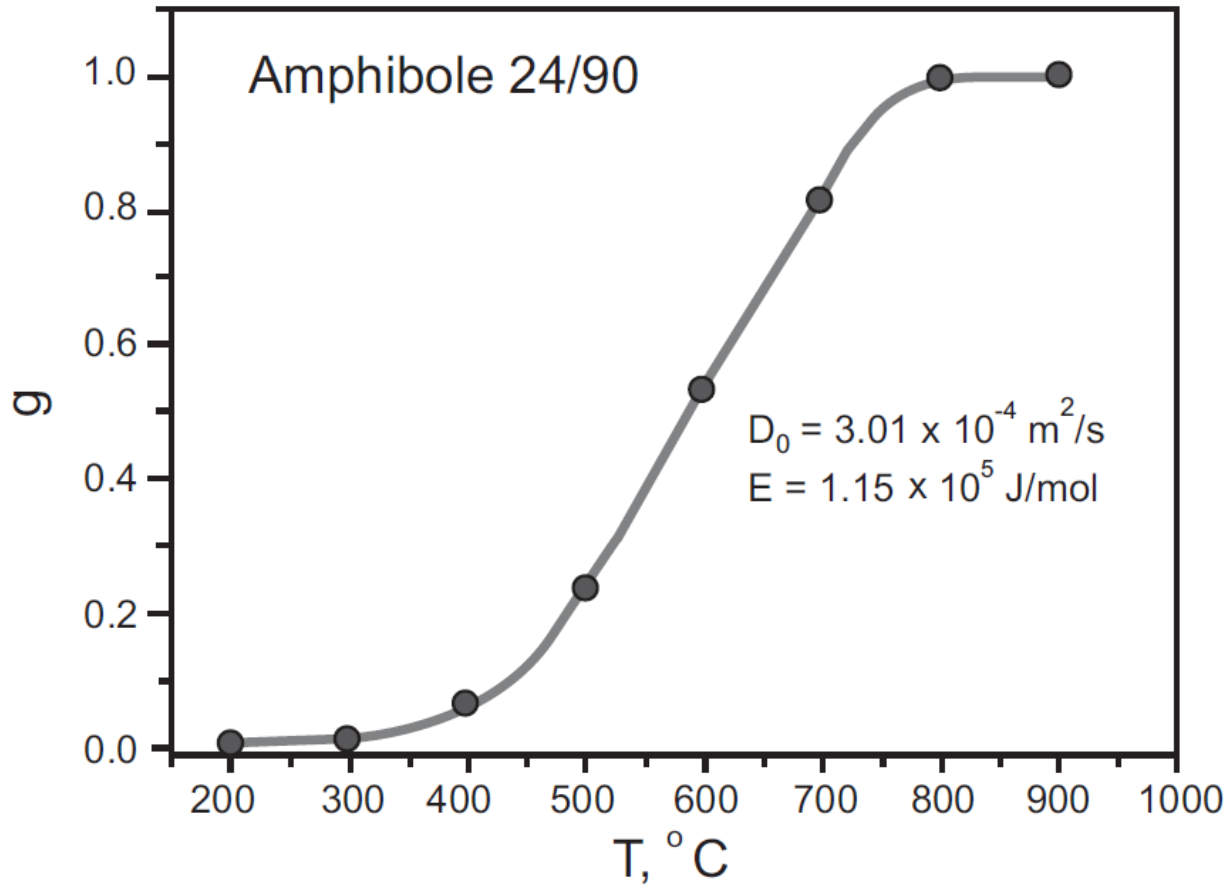

Figure 7

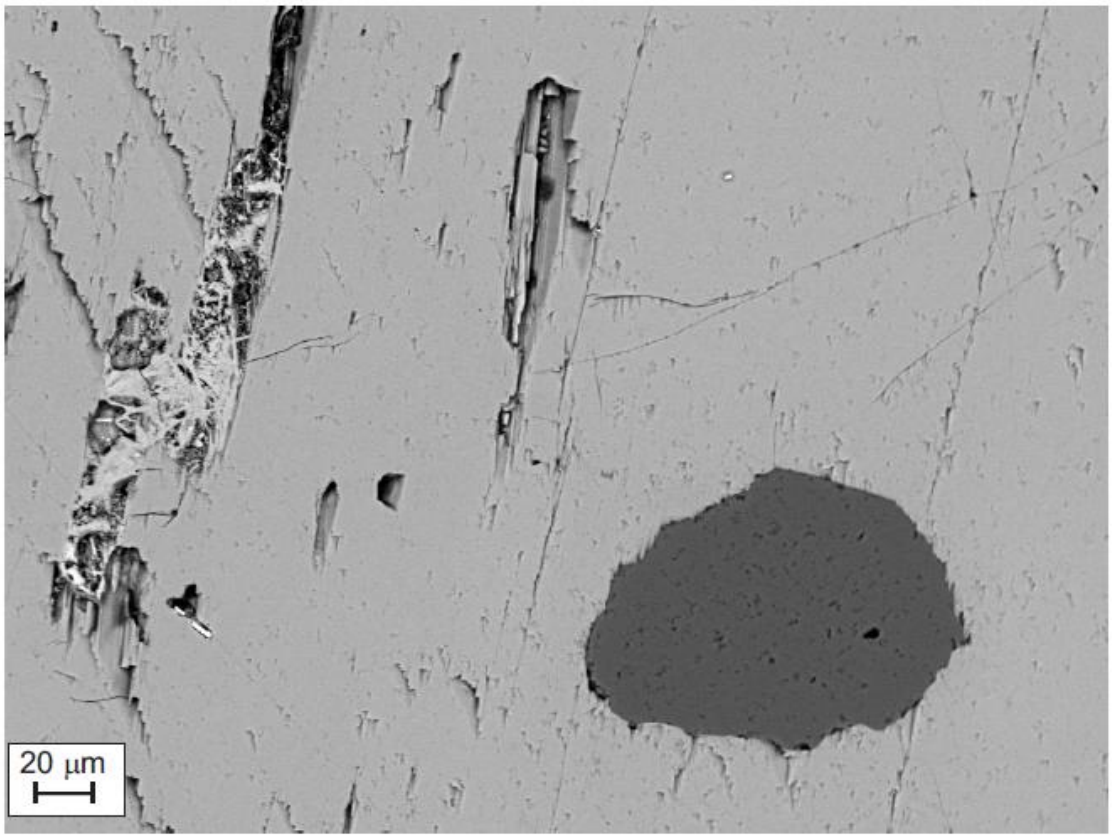

Figure 8

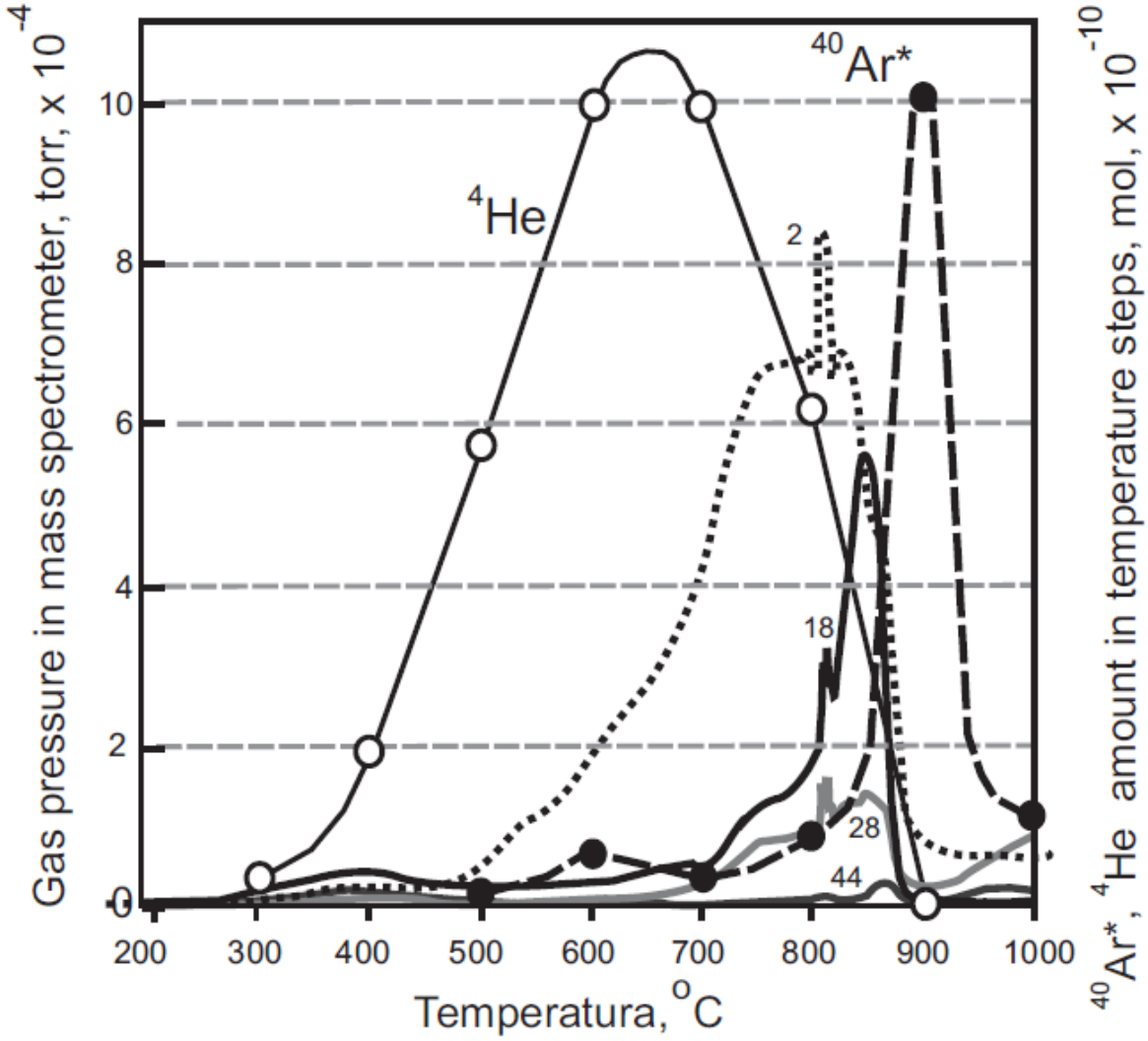

Figure 9

Table 1. U, Th and He isotopes in Rapakivi granite (Karelia) and several magmatic and metamorphic rocks (Kola Peninsula) and in amphibole separates from these rocks.

Rock name	Age	WR	Am/WR	WR	Am/WR	WR		Reference
		^4He	$\frac{^4He_{AM}}{^4He_{WR}}$	^3He	$\frac{^3He_{AM}}{^3He_{WR}}$	U	Th	$\frac{^4He_M}{^4He_C}$
	Ga	nmol g^{-1}		mol g^{-1}		μg g^{-1}	μg g^{-1}	m_4
Plagio-pyroxenite	2.8	12.1	2.4	2.19×10^{-15}	2.4	1.0	3.4	0.35	Kamensky et al., 1990
Metagabbro-norite	2.8	8.66	2.7	1.47×10^{-15}	3.4	1.0	2.7	0.27	Kamensky et al., 1990
Metagabbro	2.8	5.27	1.7	2.63×10^{-16}	1.0	1.2	3.7	0.13	Kamensky et al., 1990
Rapakivi granite	1.6	3.79	4.3	5.49×10^{-17}	13	6.7	35	0.027	Gerling et al., 1976
Diorite-gneiss	2.0	6.47	8.6	1.43×10^{-15}	7.8	1.3	6.0	0.19	Tolstikhin et al., 1978
Alkaline granite	2.7	2.99	1.2	7.48×10^{-16}	20	5.0	2.0	0.017	Vetrin et al., 1999
ibid	2.7	4.60	12	1.38×10^{-15}	15	8.0	4.0	0.015	Vetrin et al., 1999
ibid	2.7	5.58	6.7	1.17×10^{-15}	17	6.0	3.0	0.024	Vetrin et al., 1999

Footnotes to Table 1.

U and Th concentrations [μg g^{-1}] and the retention parameters (m_4) have been determined only in three amphibole separates from samples of plagio-pyroxenite (U = 0.5, Th=2.7, m_4 =1.4), Rapakivi granite (3.5, 12.7, 0.27), and diorite-gneiss (1.0, 9.0, 1.5). Note that m_4 exceeds 1 in two of three amphibole separates, whereas in the whole rock samples m_4 is always <1.

Table 2. Chemical composition of amphiboles separated from alkaline granites, Ponoy massif, Kola Peninsula

Com-ponent	Sample numbers 23/90	28/90
SiO_2	48.77	48.96
TiO_2	1.31	0.98
Al_2O_3	2.80	2.55
Fe_2O_3	12.04	11.88
FeO	22.21	22.48
MnO	0.49	0.49
MgO	0.29	0.30
CaO	2.16	1.75
Na_2O	6.19	6.50
K_2O	1.53	1.46
H_2O^-	0.25	0.19
H_2O^+	1.31	1.44
F	0.69	0.72
Cl	0.07	0.08
P_2O_5	0.09	0.07
Li_2O	0.18	0.28
Rb_2O	0.0063	0.0032
Cs_2O	0.0008	0.0005
Total	100	99.7

Table 3. Helium, argon isotopes extracted by fusion, step heating (upper bolded line) and crushing (in brackets) and Li and K concentrations in amphiboles, separated from the alkaline granites, the Ponoy massif, Kola Peninsula.

Sam-ple	^{4}He, $\times 10^{-8}$ mol g^{-1}	$\frac{^3He}{^4He}$ $\times 10^{-6}$	Li μg g^{-1}	$\frac{^3He_{MEAS}}{^3He_{CAL}}$	^{40}Ar $\times 10^{-9}$ mol g^{-1}	$\frac{^{40}Ar}{^{36}Ar}$	^{40}Ar* $\times 10^{-9}$ mol g^{-1}	$\frac{^4He}{^{40}Ar^*}$	K % wt	$\frac{\Delta^{40}Ar^*}{^{40}Ar^*_{CAL}}$
1	2	3	4	5	6	7	8	9	10	11
24/90	**1.90(0.07)**	**1.18**	**1210**	**0.36**	**8.30**	**1290**	**6.34(0.7)**	**3**	**1.32**	**-**
22/90	3.59	0.41	846	0.34	8.17	24150	8.07	4.45	1.21	0.23
29/90	5.68	0.36	987	0.41	6.79	19610	6.68	8.50	0.72	0.72
31/90	3.75	0.54	1081	0.35	8.30	56370	8.26	4.53	0.94	0.63
28/90	1.68(0.030)	2.06	1316	0.52	8.21	5730	7.79	2.15	1.04	0.38
23/90	2.31(0.071)	0.61	846	0.33	8.35	12170	8.15	2.84	1.09	0.38
24/90	2.63(0.089)	1.22	1269	0.50	8.70	20320	8.58	3.07	1.09	0.45
27/90	1.12	0.86	658	0.29	7.19	16630	7.06	1.58	1.10	0.18
30/90	5.58	0.39	1457	0.30	5.80	10900	5.65	9.88	0.94	0.11
AV	**3.13**	**0.81**	**1058**	**0.36**	**7.76**	**20735**	**7.40**	**5**	**1.0**	**0.39**
STD	**1.6**	**0.6**	**270**	**0.08**	**1.0**	**15000**	**1.0**	**3**	**0.15**	**0.21**

Footnotes to Table 2.

Amphiboles have been separated from: microcline-quartz-amphibole- vein 24/90 (upper bolded line, this study); granites, 22/90, 29/90 and 31/90, pegmatite 28/90 and 23/90, quartz vein 24/90, 27/90 and 30/90 (presented for comparison from Vetrin et al., 1999). Data in the upper line (in bold, sample 24/90) are the least precise because they were obtained as a sum of 9 step heating measurements.

Amounts of ^{4}He and ^{40}Ar* extracted by GI crushing are shown in brackets in columns 2 and 8, respectively; the average values for 2 runs is presented in the upper bolded line; a relatively large fraction of ^{40}Ar*, ≈ 11 % (average from two experiments), and only ≈ 3 % of ^{4}He (five experiments) were extracted. For the sample **24/90** this gives ^{4}He / ^{40}Ar* ≈ 0.1 in gases extracted by crushing, which presumably occupy fluid inclusions; this value is well below the average measured bulk ratio, 5 (column 9), and the bulk production ratio, 15, calculated from (U+Th)/K ratio in sample **24/90**.

Column 11 presents fraction $\Delta^{40}Ar^* = (^{40}Ar^*_{MEAS} - ^{40}Ar^*_{CALC}) / ^{40}Ar^*_{CALC}$, where $^{40}Ar^*_{MEAS}$ is measured concentrations shown in column 8; $^{40}Ar^*_{CALC}$ is calculated from ^{40}K decay (K in column 10) during post-metamorphic period 1802 Ga (Section 3).

Concentrations of U and Th are available for samples 24/90 (7.7 and 7.2 μg g^{-1}) and 28/90 (5 and 30 μg g^{-1}, respectively). Assuming the accumulation time to be equal to the metamorphism age, 1802 Ma, the calculated ^{4}He* concentrations in these samples are equal to 1.08×10^{-7} and 1.31×10^{-7} mol g^{-1}, respectively, and the average m_4 for these sample is 0.16 ± 0.02. This is at least by a factor of ≈ 2 to 3 below the m_3 values shown in this Table.

Table 4. Amounts of He and Ar isotopes in gas fractions extracted by step wise heating of amphibole 24/90 (separated from quartz-fieldspar dike, alkaline granites, the Ponoy massif, Kola Peninsula, sample weight 0.243 g)

Tempera -ture, ^{O}C	^{4}He $\times 10^{-10}$ mol	^{3}He $\times 10^{-16}$ mol	40Ar* $\times 10^{-10}$ mol
200	0.001	0	0
300	0.032	0.04	0.076
400	0.002	0.002	0
500	0.43	0.17	0.14
600	7.2	4.86	0.61
700	15.2	16.7	0.29
800	22.2	31.1	0.83
900	1.1	1.8	10.9
1000	0.005	0.007	1.62
1200	0.007	0.006	0.87
1400	0.001	0	0
Total	**46.2**	**54.7**	**15.5**

Table 5. Diffusion parameters for amphiboles from the Kola Peninsula in comparison with published data.

Sample	E , J/mol	R^2/D_0, sec	Source
Amphibole 24/90, Ponoy massif	1.14e+5	3.3×10^{-3}	This work
Amphibole, Keivy massif	7.65e+4	4.7×10^{-1}	This work
Hornblende LK-5	1.04E+5	5.9×10^{-2}	Lippolt and Weigel (1988)
Hornblende SAU B	1.20E+5	3.3×10^{-2}	Lippolt and Weigel (1988)
Pargasite	1.13E+5	1.5×10^{-3}	Jackson et al. (2016)
Richterite	1.21E+5	4.2×10^{-3}	Jackson et al. (2016)
Tremolite	1.16E+5	7.4×10^{-2}	Jackson et al. (2016)
Actinolite	1.01E+5	5.7×10^{-1}	Jackson et al. (2016)